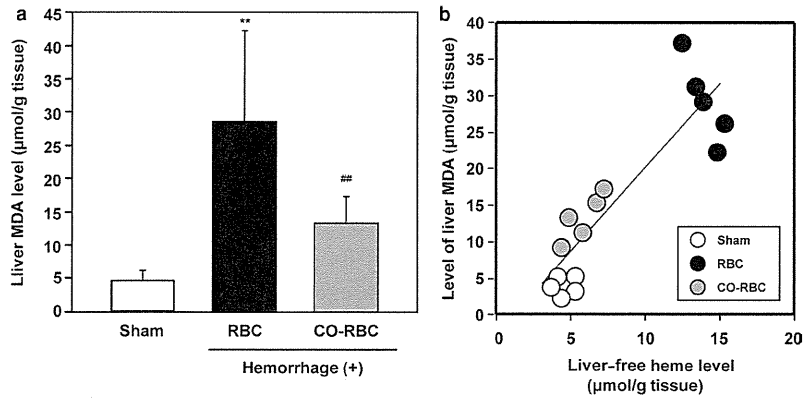

Figure 4. (a) Level of MDA in liver in sham and hemorrhagic shock rats at 1 h after resuscitation by RBC or CO-RBC. (b) Relationship between the level of free heme and MDA in liver to sham (opened circles) and hemorrhagic shock rats at 1 h after resuscitation by RBC (closed circles) or CO-RBC (gray circles). The values are means ± SD ($n = 5$). $^{**}p < 0.01$ versus sham group. $^{\#\#}p < 0.01$ versus RBC group. The linear regression of logarithmic values was calculated using the least-squares method ($y = 2.29x-2.74$, $r = 0.89$, $p < 0.01$).

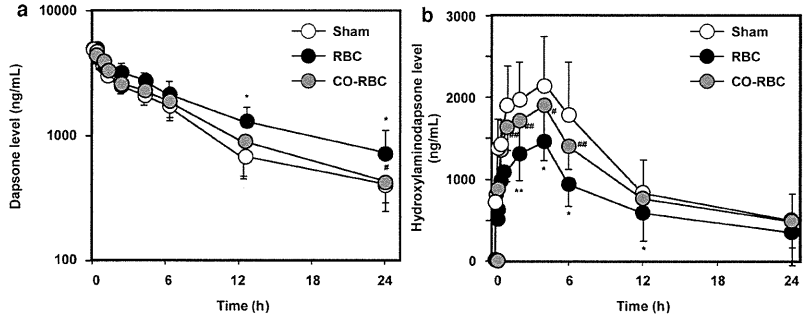

Figure 5. Plasma concentration of (a) dapsone and (b) hydroxylaminodapsone after an i.v. administration of dapsone to sham (opened circle) and hemorrhagic shock rats at 1 h after resuscitation by RBC (closed circle) or CO-RBC (gray circle). Each point represents the mean ± SD ($n = 5$). The values are means ± SE ($n = 5$). $^{*}p < 0.05$, $^{**}p < 0.01$ versus sham group. $^{\#}p < 0.05$, $^{\#\#}p < 0.01$ versus RBC group.

heme level in liver was found at 1 h after resuscitation (data not shown: $y = 6.93x-10.3$, $r = 0.97$, $p < 0.01$). These data indicate that the increased free heme levels in the liver are strongly related to tissue injury and tissue oxidation.

Effect of Decreased CYP Expression After Hemorrhage and Resuscitation on the Pharmacokinetics of Dapson

Cytochrome P450 has a broad range of functions, including the metabolism and detoxification of endogenous and exogenous substances.[21] As the majority of CYP is located in the liver, any alteration in hepatic CYP levels or activity would constitute a major influence on the disposition of drugs. Therefore, we next addressed the issue of whether changes in the levels of CYP protein directly affected the pharmacokinetics of the process using dapsone, which is metabolized by the multiple CYP isoforms. Figure 5a shows the time course for the plasma concentration of dapsone in the sham, RBC, and CO-RBC groups resuscitation. The plasma concentrations of dapsone were substantially elevated in the RBC resuscitation group, whereas the profile for the concentrations in the CO-RBC resuscitation groups was similar to that for the sham group. Compared with the sham group, the area under the blood concentration–time curve (AUC) for dapson in the RBC resuscitation group was significantly increased, whereas the results for the CO-RBC resuscitation group were similar to those for the sham group (Table 1).

Moreover, accompanying the changes in the plasma concentration of dapson, the plasma concentrations of the hydroxylaminodapsone, a metabolite derived from dapson, were decreased in the RBC resuscitation group, whereas the profile for the concentrations in the CO-RBC resuscitation groups was similar to that for the sham group (Fig. 5b). These data confirm that the significant alternations in hepatic CYP expressions by hemorrhage and resuscitation were major contributors to the changes in the CYP metabolized drugs.

DISCUSSION

The clinical indications for RBC transfusion are unquestionable during a massive hemorrhage. However, hepatic ischemia–reperfusion injury, a major complication of hemorrhage and resuscitation by RBC, is a serious and common adverse event that can ultimately lead to liver failure. Therefore, the development of a novel resuscitable fluid without hepatic ischemia–reperfusion injury would contribute to further advances in emergency medical care. In the present study, we evaluated the effect of CO-RBC transfusion, a novel promising RBC transfusion alternative, on protection against hepatic ischemia–reperfusion injury and CYP expression. In addition, we further found that free heme, derived from CYP, that had been destroyed by ischemia–reperfusion after hemorrhage and resuscitation was strongly associated with hepatic injury and

Table 1. Pharmacokinetic Parameters for Dapsone After Intravenous Injection to Sham Rats and Hemorrhagic Shock Rats Resuscitated by Red Blood Cell (RBC) or Carbon Monoxide-bound Red Blood Cells (CO-RBC)

	$t_{1/2}$ (h)	k_e ($\times 10^{-3}$ min^{-1})	AUC (h × ng/mL)	CL (L/h)	V_d (L)
Sham	7.3 ± 1.5	1.7 ± 0.4	30.6 ± 6.7	0.18 ± 0.04	1.03 ± 0.03
RBC	11.5 ± 2.7*	1.0 ± 0.2**	48.1 ± 8.5*	0.11 ± 0.02	1.04 ± 0.02
CO-RBC	8.3 ± 0.6	1.4 ± 0.1	36.4 ± 8.3	0.15 ± 0.03	1.04 ± 0.02

Values are means ± SD ($n = 5$). *$p < 0.05$, **$p < 0.01$ versus sham group.

oxidation. Furthermore, inhibiting alterations in CYP protein levels by CO-RBC significantly suppressed the changes in the pharmacokinetic properties of a CYP-metabolizing drug and its metabolite, dapson and hydroxylaminodapsone, respectively.

Zuckerbraun et al.[22] reported on the effect of inhaled CO at a low concentration following hemorrhagic shock and resuscitation on multiple organ injury, and reported that inhaled CO suppressed myeloperoxidase levels in the lung and tissue injury in both liver and small intestine. In addition, Morita and coworkers[23,24] also reported that inhaled CO at a low concentration ameliorated hemorrhagic shock and RBC resuscitation-induced acute lung injury in rats. The findings reported herein clearly demonstrate that the increased AST and ALT was suppressed after hemorrhagic shock and CO-RBC resuscitation compared with RBC resuscitation (Fig. 1). This might be because of the slow gas exchange between oxygen and CO, which could attenuate ischemia–reperfusion injury. Although it is not clear that CO-RBC resuscitation after hemorrhagic shock had a protective effect on other organs, CO-RBC resuscitation appeared to attenuate the multiple organ injury induced by hemorrhage and RBC resuscitation as well as in the liver. In fact, it was reported that plasma enzyme levels of lactate dehydrogenase and its isozymes were significantly lower in CO-RBC resuscitation groups than in the RBC resuscitation group.[11] Clearly, further studies of this issue will be needed to demonstrate variety and utility of CO-RBC as a novel resuscitable fluid in terms of limiting multiple organ injury.

It is well known that hemorrhagic shock is a generalized systemic ischemic state, and hemorrhagic shock and RBC resuscitation induces systematic reperfusion injury.[1] In short, hemorrhagic shock caused by blood loss is the inability of the body to maintain adequate organ perfusion, which means that systemic organs are under low-oxygen conditions. To replace circulating volume, and to recover oxygen carrying capacity, resuscitation with RBC transfusion is performed, which induce reperfusion injury. However, in this study, we found that CO-RBC resuscitation decreased hepatic-free heme levels by protecting against the destruction of CYP after hemorrhagic shock and resuscitation (Fig. 3). It is known that free heme can facilitate the generation of ROS, via the Fenton reaction,[20] resulting in the induction of tissue damage. In fact, the findings of this study showed a significant correlation between hepatic injury, such as plasma ALT and hepatic MDA, and free heme levels in the liver at 1 h after hemorrhagic shock and resuscitation. Regarding the mechanisms underlying the protective effects of CO in organ ischemia–reperfusion injury, Kim et al.[25] reported that inhaled CO protected against hepatic warm ischemia–reperfusion injury by inhibiting the production of glycogen synthase kinase-3 through Ser9 phospholylation mediated by the activation of phosphatidylinositol 3-kinase/Akt, leading to anti-inflammation. In addition, Wei et al.[26] reported that treatment with CORM resulted in the upregulation of the protein expression of Bcl-2 and the downregulation of caspase-3 activation, leading to antiapoptosis, in a rat model of hepatic ischemia–reperfusion.[26] As CO donors, such as CO inhalation and CORMs, have been demonstrated to exhibit anti-inflammation and antiapoptosis effects, CO-RBC resuscitation would also be expected to exert such effects in hemorrhagic shock model rats, resulting in the suppression of hepatic ischemia–reperfusion injury. Indeed, Cabrales et al.[10] showed that CO-RBC resuscitation significantly decreased the number of apoptotic cells compared with RBC resuscitation using a rodent model of 50% hemorrhagic shock. Furthermore, the maintenance of hepatic microcirculatory flow after ischemia of the liver derived from hemorrhagic shock is also essential in preventing the development of hepatic dysfunction, because hemorrhagic shock is caused perturbation in the hepatic microcirculation. The effect of endogenous CO on hepatic vascular tone was previously demonstrated by Suematsu et al.[27,28] using perfused rat livers. Even in hemorrhagic shock and resuscitation, it was demonstrated that endogenously generated CO acts to maintain sinusoidal perfusion, the mitochondrial redox state, and the secretary function of the liver.[29]

Therefore, exogenous CO derived from CO-RBC may attenuate hepatic ischemia–reperfusion injury by functioning as a modulator of vascular perfusion in the liver.

Another concern of note in the destruction of CYP was the influence on the disposition and pharmacological activities of CYP-metabolizing drugs. Previously, we realized that CO-RBC resuscitation suppressed changes in CYP isoform levels (CYP 1A2, 2C11, 2E1, and 3A2) compared with RBC resuscitation in hemorrhagic shock model rats, and consequently, such an inhibition in the alteration of CYP isoform levels by CO-RBC significantly suppressed the changes in the pharmacokinetic of substrate drugs [caffeine (1A2), tolbutamide (2C11), chlorzoxazone (2E1), and midazolam (3A2)] for each P450 isoform.[9] In the present study, we found marked reductions in the levels of total hepatic CYP associated with RBC resuscitation, and these reductions were significantly inhibited in the case of CO-RBC resuscitation to values approaching the sham levels (Fig. 3). Correspondingly, after CO-RBC resuscitation, not only dispositions of the nonisoform-specific CYP substrate drug but also its metabolite, dapson and hydroxylaminodapsone, respectively, remained at levels similar to those found for the sham group (Fig. 5 and Table 1). In a previous study, Harbrecht et al.[30] examined the disposition of drugs metabolized by isoforms of CYP in critically ill trauma patients after RBC transfusions, and reported that their metabolic activities by CYP were decreased. In intensive care units of emergency conditions, CYP-metabolizing drugs, such as fentanyl and propofol, are frequently employed in the treatment for maintaining circulatory dynamics and for preventing complications arising as the result of hemorrhagic shock and resuscitation. Therefore, maintaining drug metabolism using CO-RBC can be of

great significance from the viewpoint of regulating the pharmacokinetic properties and pharmacodynamic action for CYP substrates, leading to achieving a safe and effective drug therapy during a massive hemorrhage and resuscitation. Indeed, we previously showed that CO-RBC resuscitation suppressed the changes in the pharmacokinetic–pharmacodynamic properties of midazolam, substrates for CYP 3A2, compared with RBC transfusion.[9] However, the issue of whether the results obtained from animal models of hemorrhagic shock would be directly applicable to humans are not entirely clear at this time. Accumulating further evidence to show that the expression of hepatic CYP proteins and CYP activity is affected in patients with hemorrhagic shock and RBC resuscitation will be needed.

From a clinical perspective, the toxicity of CO-RBC is of concern because of the potential for CO poisoning.[31] Cabrales et al.[10] and Sakai et al.[11] prepared CO-RBC under the same conditions as were used in the present study, and compared its resuscitative effect and safety with RBC transfusion using a rodent model of 50% hemorrhagic shock. We used a 40% hemorrhagic shock rat model, and also observed that the CO-RBC resuscitative fluid group survived, with no signs of hypoxia or abnormal behavior after resuscitation. Although these results demonstrate the safety and utility of CO-RBC as a resuscitative fluid, the bleeding volume was fixed at 40% or 50% in these studies. In actual clinical settings, a fluid transfusion involving RBC to an extent that the entire circulating blood volume is exceeded is necessary, because some hemorrhages are uncontrollable. Exposure to large concentrations of CO increased serum carboxyhemoglobin levels, which can cause several types of toxicity such as nausea, vomiting, convulsions, and ultimately death.[31] Therefore, it will be necessary to investigate the safety and efficacy of CO-RBC transfusions as a resuscitative fluid in massive hemorrhage conditions in which the circulatory volume is exceeded.

CONCLUSIONS

Hepatic ischemia–reperfusion injury is induced by not only systemic hemorrhagic shock but also various local types of ischemia, such as surgical hepatectomy and liver transplantation. Under these conditions, a transfusion is usually required. In addition, there were many reports demonstrating that treatment with inhaled CO or CORMs have cytoprotective effects on ischemia–reperfusion injuries in other organs, such as the kidney and heart.[2,3] These protective effects of CO-RBC against hepatic ischemia–reperfusion injury constitute an excellent prognosis after pathological situations involving both the systemic and the local ischemia. As the benefit of CO as a therapeutic agent has already been revealed preclinically in animal models of various human diseases related to ROS and inflammation,[32] CO-RBC has the potential for use in novel blood transfusions without the limitations that are currently associated with RBC transfusions, and for having promising new pharmaceutics as CO donor that would arrest ROS and inflammation-related disorders.

ACKNOWLEDGMENT

This work was supported by Grant-in-Aid for Scientific Research from Japan Society for the Promotion of Science (JSPS) (KAKENHI 18390051 and 22790162).

REFERENCES

1. Allan PF, Bloom BB, Wanek S. 2011. Reversal of hemorrhagic shock-associated hepatic ischemia-reperfusion injury with N-acetylcysteine. Mil Med 176(3):332–335.
2. Caumartin Y, Stephen J, Deng JP, Lian D, Lan Z, Liu W, Garcia B, Jevnikar AM, Wang H, Cepinskas G, Luke PP. 2011. Carbon monoxide-releasing molecules protect against ischemia–reperfusion injury during kidney transplantation. Kidney Int 79(10):1080–1089.
3. Nakao A, Kaczorowski DJ, Wang Y, Cardinal JS, Buchholz BM, Sugimoto R, Tobita K, Lee S, Toyoda Y, Billiar TR, McCurry KR. 2010. Amelioration of rat cardiac cold ischemia/reperfusion injury with inhaled hydrogen or carbon monoxide, or both. J Heart Lung Transplant 29(5):544–553.
4. Tomiyama K, Ikeda A, Ueki S, Nakao A, Stolz DB, Koike Y, Afrazi A, Gandhi C, Tokita D, Geller DA, Murase N. 2008. Inhibition of Kupffer cell-mediated early proinflammatory response with carbon monoxide in transplant-induced hepatic ischemia/reperfusion injury in rats. Hepatology 48(5):1608–1620.
5. Brouard S, Berberat PO, Tobiasch E, Seldon MP, Bach FH, Soares MP. 2002. Heme oxygenase-1-derived carbon monoxide requires the activation of transcription factor NF-kappa B to protect endothelial cells from tumor necrosis factor-alpha-mediated apoptosis. J Biol Chem 277(20):17950–17961.
6. Otterbein LE, Bach FH, Alam J, Soares M, Tao Lu H, Wysk M, Davis RJ, Flavell RA, Choi AM. 2000. Carbon monoxide has anti-inflammatory effects involving the mitogen-activated protein kinase pathway. Nat Med 6(4):422–428.
7. Foresti R, Bani-Hani MG, Motterlini R. 2008. Use of carbon monoxide as a therapeutic agent: Promises and challenges. Intensive Care Med 34(4):649–658.
8. Omaye ST. 2002. Metabolic modulation of carbon monoxide toxicity. Toxicology 180(2):139–150.
9. Ogaki S, Taguchi K, Watanabe H, Otagiri M, Maruyama T. 2013. Carbon monoxide-bound red blood cells protect red blood cell transfusion-induced hepatic cytochrome P450 impairment in hemorrhagic-shock rats. Drug Metab Dispos 41(1):141–148.
10. Cabrales P, Tsai AG, Intaglietta M. 2007. Hemorrhagic shock resuscitation with carbon monoxide saturated blood. Resuscitation 72(2):306–318.
11. Sakai H, Horinouchi H, Tsuchida E, Kobayashi K. 2009. Hemoglobin vesicles and red blood cells as carriers of carbon monoxide prior to oxygen for resuscitation after hemorrhagic shock in a rat model. Shock 31(5):507–514.
12. Taguchi K, Iwao Y, Watanabe H, Kadowaki D, Sakai H, Kobayashi K, Horinouchi H, Maruyama T, Otagiri M. 2011. Repeated injection of high doses of hemoglobin-encapsulated liposomes (hemoglobin vesicles) induces accelerated blood clearance in a hemorrhagic shock rat model. Drug Metab Dispos 39(3):484–489.
13. Taguchi K, Maruyama T, Iwao Y, Sakai H, Kobayashi K, Horinouchi H, Tsuchida E, Kai T, Otagiri M. 2009. Pharmacokinetics of single and repeated injection of hemoglobin-vesicles in hemorrhagic shock rat model. J Control Release 136(3):232–239.
14. Sakai H, Masada Y, Horinouchi H, Yamamoto M, Ikeda E, Takeoka S, Kobayashi K, Tsuchida E. 2004. Hemoglobin-vesicles suspended in recombinant human serum albumin for resuscitation from hemorrhagic shock in anesthetized rats. Crit Care Med 32(2):539–545.
15. Ishima Y, Chen D, Fang J, Maeda H, Minomo A, Kragh-Hansen U, Kai T, Maruyama T, Otagiri M. 2012. S-Nitrosated human serum albumin dimer is not only a novel anti-tumor drug but also a potentiator for anti-tumor drugs with augmented EPR effects. Bioconjug Chem 23(2):264–271.
16. Omura T, Sato R. 1964. The carbon monoxide-binding pigment of liver microsomes. I. Evidence for its hemoprotein nature. J Biol Chem 239:2370–2378.
17. Kwadijk S, Torano JS. 2002. High-performance liquid chromatographic method with ultraviolet detection for the determination of

dapsone and its hydroxylated metabolite in human plasma. Biomed Chromatogr 16(3):203–208.
18. Yamaoka K, Tanigawara Y, Nakagawa T, Uno T. 1981. A pharmacokinetic analysis program (multi) for microcomputer. J Pharmacobiodyn 4(11):879–885.
19. Kan WH, Hsu JT, Schwacha MG, Choudhry MA, Raju R, Bland KI, Chaudry IH. 2008. Selective inhibition of iNOS attenuates trauma-hemorrhage/resuscitation-induced hepatic injury. J Appl Physiol (1985) 105(4):1076–1082.
20. Jomova K, Valko M. 2011. Advances in metal-induced oxidative stress and human disease. Toxicology 283(2–3):65–87.
21. Morgan ET. 2001. Regulation of cytochrome P450 by inflammatory mediators: Why and how? Drug Metab Dispos 29(3):207–212.
22. Zuckerbraun BS, McCloskey CA, Gallo D, Liu F, Ifedigbo E, Otterbein LE, Billiar TR. 2005. Carbon monoxide prevents multiple organ injury in a model of hemorrhagic shock and resuscitation. Shock 23(6):527–532.
23. Kanagawa F, Takahashi T, Inoue K, Shimizu H, Omori E, Morimatsu H, Maeda S, Katayama H, Nakao A, Morita K. 2010. Protective effect of carbon monoxide inhalation on lung injury after hemorrhagic shock/resuscitation in rats. J Trauma 69(1):185–194.
24. Kawanishi S, Takahashi T, Morimatsu H, Shimizu H, Omori E, Sato K, Matsumi M, Maeda S, Nakao A, Morita K. 2013. Inhalation of carbon monoxide following resuscitation ameliorates hemorrhagic shock-induced lung injury. Mol Med Rep 7(1):3–10.
25. Kim HJ, Joe Y, Kong JS, Jeong SO, Cho GJ, Ryter SW, Chung HT. 2013. Carbon monoxide protects against hepatic ischemia/reperfusion injury via ROS-dependent Akt signaling and inhibition of glycogen synthase kinase 3beta. Oxid Med Cell Longev 2013:306421.
26. Wei Y, Chen P, de Bruyn M, Zhang W, Bremer E, Helfrich W. 2010. Carbon monoxide-releasing molecule-2 (CORM-2) attenuates acute hepatic ischemia reperfusion injury in rats. BMC Gastroenterol 10:42.
27. Suematsu M, Goda N, Sano T, Kashiwagi S, Egawa T, Shinoda Y, Ishimura Y. 1995. Carbon monoxide: An endogenous modulator of sinusoidal tone in the perfused rat liver. J Clin Invest 96(5):2431–2437.
28. Suematsu M, Kashiwagi S, Sano T, Goda N, Shinoda Y, Ishimura Y. 1994. Carbon monoxide as an endogenous modulator of hepatic vascular perfusion. Biochem Biophys Res Commun 205(2):1333–1337.
29. Pannen BH, Kohler N, Hole B, Bauer M, Clemens MG, Geiger KK. 1998. Protective role of endogenous carbon monoxide in hepatic microcirculatory dysfunction after hemorrhagic shock in rats. J Clin Invest 102(6):1220–1228.
30. Harbrecht BG, Frye RF, Zenati MS, Branch RA, Peitzman AB. 2005. Cytochrome P-450 activity is differentially altered in severely injured patients. Crit Care Med 33(3):541–546.
31. Weaver LK. 2009. Clinical practice. Carbon monoxide poisoning. N Engl J Med 360(12):1217–1225.
32. Motterlini R, Otterbein LE. 2010. The therapeutic potential of carbon monoxide. Nat Rev Drug Discov 9(9):728–743.

Supplemental material to this article can be found at:
http://jpet.aspetjournals.org/content/suppl/2014/11/14/jpet.114.219493.DC1.html

1521-0103/352/2/244–257$25.00
THE JOURNAL OF PHARMACOLOGY AND EXPERIMENTAL THERAPEUTICS

http://dx.doi.org/10.1124/jpet.114.219493
J Pharmacol Exp Ther 352:244–257, February 2015

Polythiol-Containing, Recombinant Mannosylated-Albumin Is a Superior CD68$^+$/CD206$^+$ Kupffer Cell–Targeted Nanoantioxidant for Treatment of Two Acute Hepatitis Models[S]

Hitoshi Maeda, Kenshiro Hirata, Hiroshi Watanabe, Yu Ishima, Victor Tuan Giam Chuang, Kazuaki Taguchi, Akihito Inatsu, Manabu Kinoshita, Motohiko Tanaka, Yutaka Sasaki, Masaki Otagiri, and Toru Maruyama

Department of Biopharmaceutics, Graduate School of Pharmaceutical Sciences (H.M., K.H., H.W., Y.I., V.T.G.C., T.M.), Center for Clinical Pharmaceutical Sciences, School of Pharmacy (H.W., Y.I., T.M.), and Department of Gastroenterology and Hepatology, Graduate School of Medical Sciences (M.T., Y.S.), Kumamoto University, Kumamoto, Japan; School of Pharmacy, Faculty of Health Sciences, Curtin Health Innovation Research Institute, Curtin University, Perth, Western Australia, Australia (V.T.G.C.); Faculty of Pharmaceutical Sciences (K.T., M.O.) and DDS Research Institute (M.O.), Sojo University, Kumamoto, Japan; and Department of Immunology and Microbiology, National Defense Medical College, Saitama, Japan (A.I., M.K.)

Received August 24, 2014; accepted November 3, 2014

ABSTRACT

Since reactive oxygen species (ROS) derived from Kupffer cells (KC), especially CD68$^+$ KC, play a key role in the induction of hepatic oxidative stress and injuries, we developed a polythiolated- and mannosylated human serum albumin (SH-Man-HSA), which functions as a novel nanoantioxidant for delivering thiol to CD68$^+$ KC. In vitro electron paramagnetic resonance coupled with pharmacokinetics and immunohistochemical studies showed that SH-Man-HSA possessed powerful radical-scavenging activity and rapidly and selectively delivered thiols to the liver via mannose receptor (CD206) on CD68$^+$ cells. SH-Man-HSA significantly improved the survival rate of concanavalin-A (Con-A)–treated mice. Moreover, SH-Man-HSA exhibited excellent hepatoprotective functions, not by decreasing tumor necrosis factor or interferon-γ production that is closely associated with Con-A–induced hepatitis, but by suppressing ROS production. Interestingly, the protective effect of SH-Man-HSA was superior to *N*-acetyl cysteine (NAC). This could be attributed to the difference in the inhibition of hepatic oxidative stress between the two antioxidants depending on their potential for thiol delivery to the liver. Similar results were also observed for acetaminophen (APAP)-induced hepatopathy models. Flow cytometric data further confirmed that an increase in F4/80$^+$/ROS$^+$ cells was dramatically decreased by SH-Man-HSA. The administration of SH-Man-HSA at 4 hours following a Con-A or APAP injection also exhibited a profound hepatoprotective action against these hepatitis models, whereas this was not observed for NAC. It can be concluded therefore that SH-Man-HSA has great potential for use in a rescue therapy for hepatopathy as a nanoantioxidant because of its ability to efficiently and rapidly deliver thiols to CD68$^+$/CD206$^+$ KC.

Introduction

Oxidative stress plays a key role in the onset and progression of various liver diseases, including viral hepatitis (Korenaga et al., 2005), autoimmune hepatitis (Moreno-Otero, 2013), alcoholic hepatopathy (Tsukamoto and Lu, 2001), and drug-induced hepatic impairment (Laskin and Laskin, 2001). Reactive oxygen species (ROS) produced upon activation of Kupffer cells (KC), and subsequent production of inflammatory cytokines, such as tumor necrosis factor (TNF)–cytokines triggered by the presence of ROS, have been shown to be involved in the progression of a number of liver pathologic conditions (Roberts et al., 2007; Jaeschke, 2011). Kinoshita et al. (2010) reported on the subclassification of KC on the basis of their surface markers and functions, namely, CD68$^+$, residential, and CD11b$^+$ KC, monocyte-derived. CD68$^+$ KC have a potent capacity to produce ROS, whereas CD11b$^+$ cells did not. Conversely, CD11b$^+$ KC have a strong capacity for the production of TNF, which was much less prominent in

This research was supported, in part, by Grant-in-Aid for Scientific Research from Japan Society for the Promotion of Science (JSPS) (KAKENHI 21390177).
dx.doi.org/10.1124/jpet.114.219493.
[S] This article has supplemental material available at jpet.aspetjournals.org.

ABBREVIATIONS: 8-OHdG, 8-hydroxy-2′-deoxyguanosine; ALT, alanine aminotransferase; APAP, acetaminophen; AST, aspartate aminotransferase; CD206, mannose receptor; Con-A, concanavalin-A; DMPO, 5,5-dimethyl-1-pyrroline l-oxide; DTNB, 5,5′-dithiobis-(2-nitrobenzoic acid); DTPA, diethylenetriamine-pentaacetic acid; EPR, electron paramagnetic resonance; GSH, glutathione; GSH/GSSG, reduced/oxidized glutathione ratio; HIF-1α, hypoxia-inducible factor-1α; HSA, human serum albumin; IFN-γ, interferon-γ; KC, Kupffer cells; KPB, potassium phosphate buffer; Man-HSA, mannosylated-HSA; NAC, *N*-acetyl cysteine; NAPQI, *N*-acetyl-*p*-benzoquinone imine; PBS, phosphate-buffered saline; POBN, α-(4-pyridyl-1-oxide)-*N*-*tert*-butylnitrone; rHSAs, recombinant HSAs; ROS, reactive oxygen species; SH-Man-HSA, polythiolated-Man-HSA; SH, thiol; TNF, tumor necrosis factor; TUNEL, terminal deoxynucleotidyl transferase dUTP nick-end labeling.

$CD68^+$ cells. Moreover, ROS produced by $CD68^+$ KC have been identified as an aggravating factor for the onset and progression of hepatitis in a concanavalin-A (Con-A)–induced hepatitis mouse model (Nakashima et al., 2008). In addition, mice that were pretreated with gadolinium chloride ($GdCl_3$), a KC inhibitor, especially $CD68^+$ cells, showed a decreased acetaminophen (APAP)-induced hepatotoxicity, possibly by suppressing the induction of oxidative stress (Laskin et al., 1995; Michael et al., 1999). This was particularly evident in the case of $CD68^+$ KC. It therefore appears that KC, especially $CD68^+$, play a major role in the progression of liver pathologic conditions. In fact, it had been shown that the intensity of KC activation, on the basis of CD68 expression, is directly correlated with the degree of disease severity in patients with alcoholic liver disease (Chedid et al., 2004). Interestingly, mannose receptors (CD206) are present on the KC surface, including $CD68^+$ (Hu et al., 2012). An effective ROS-scavenging agent that can be delivered to $CD68^+$ KC in the liver through CD206 would therefore be predicted to result in promising therapeutic outcomes. However, as far as we know, no carrier that targets $CD68^+/CD206^+$ KC is currently available.

Human serum albumin (HSA) is a simple protein with no oligosaccharide chain structures. However, the insertion of a consensus sequence for an oligosaccharide chain into the albumin gene results in the production of a protein that contains an oligosaccharide chain, as in some reported genetic variants (Minchiotti et al., 2001). Using three HSA variants—Albumin Dalakarlia, Casebrook, and Redhill (Kragh-Hansen et al., 2001)—as a template for designing a recombinant glycosylated-HSA, we recently succeeded, employing a yeast expression system, in producing a recombinant mannosylated-HSA (Man-HSA) containing a biosynthetic oligosaccharide chain with a high content of 12 mannose residues per HSA molecule (Supplemental Fig. 1) (Hirata et al., 2010). Therefore, Man-HSA would be anticipated to be efficiently distributed to $CD68^+$ KC via CD206.

Antioxidants containing a thiol (SH) group, such as glutathione (GSH) and *N*-acetyl cysteine (NAC), possess excellent ROS-scavenging activities (Saito et al., 2010). In fact, NAC is currently the only remedy available for the treatment of APAP-induced hepatotoxicity (Lee et al., 2008). Hence, polythiolated-Man-HSA (SH-Man-HSA), produced by introducing SH groups into Man-HSA, has the potential to function as a novel nanoantioxidant that targets ROS derived from KC, especially $CD68^+/CD206^+$ and, thereby, as a candidate rescue therapy for both acute and chronic hepatopathy.

Materials and Methods

Animals. Male C57BL/6 mice (8 weeks old) were purchased from Japan SLC (Shizuoka, Japan). All animal experiments were conducted in accordance with the guidelines of Kumamoto University for the care and use of laboratory animals.

Reagents. DTPA (diethylenetriamine-pentaacetic acid) and DTNB [5,5′-dithiobis (2-nitrobenzoic acid)] were obtained from Dojindo Laboratories (Kumamoto, Japan). DMPO (5,5-dimethyl-1-pyrroline *N*-oxide) and POBN [α-(4-pyridyl-1-oxide)-*N*-*tert*-butylnitrone] were purchased from Alexis Biochemicals (Lausen, Switzerland). All other chemicals were of the highest analytical grade available.

Production and Purification of Recombinant HSAs. The protocol used to express the recombinant HSAs (rHSAs), Man-HSA and HSA, by *Pichia pastoris* was a modification of a previously published procedure (Hirata et al., 2010). The eluted rHSAs were deionized and defatted by charcoal treatment, freeze-dried, and then stored at −80°C until used. Sample purity was estimated by a density analysis of the Coomassie brilliant blue–stained protein bands on 10% SDS-PAGE gels. The rHSAs were estimated to be more than 97% pure. Matrix-assisted laser desorption/ionization–time of flight mass spectroscopy analysis revealed that approximately 12 mannose (*N*-acetyl glucosamine = 2) units are present in the glycan chain structure of the Man-HSA (Supplemental Fig. 1).

Synthesis of SH-rHSAs and Determination of Thiolation Efficiency. Terminal SH groups were added to the rHSAs molecule by incubating 0.15 mM rHSAs with 8 mM 2-iminothiolane in 100 mM potassium phosphate buffer (KPB) containing 0.5 mM DTPA, pH 7.8, for 1 hour at room temperature (Katayama et al., 2008). The amount of SH groups in the SH-rHSAs was quantified using the DTNB method. First, 20-μl aliquots of SH-rHSAs solution and reduced glutathione (standard) were incubated in a 96-well plate with 0.2 ml of 100 mM KPB, pH 7.0, containing 1 mM DTPA and 0.5 mM DTNB, for 15 minutes at room temperature. The absorbance was then measured at 405 nm. The number of SH groups attached to Man-HSA or HSA was estimated to be 7.52 ± 0.01 mol SH/mol Man-HSA or 7.82 ± 0.02 mol SH/mol HSA, respectively (Supplemental Fig. 2B).

Scavenging Activity of SH-Man-HSA against ·OH Generated by H_2O_2/UV System. The reaction solution contained 100 μM DTPA, 9 mM DMPO, and 500 μM H_2O_2 in the absence or presence of 75 μM HSA, Man-HSA or SH-Man-HSA in phosphate-buffered saline (PBS) (pH 7.4). After the sample was irradiated with UV (254 nm) for 1 minute in the electron paramagnetic resonance (EPR) flat cell, EPR spectra were measured immediately.

Pharmacokinetic Analysis of SH-Man-HSA. SH-Man-HSA was radiolabeled with ^{111}In using the bifunctional chelating reagent DTPA anhydride according to the method of Hnatowich et al. (1982). Mice received tail vein injections of ^{111}In-labeled SH-Man-HSA in saline, at a dose of 10.0 nmol SH/kg. In the early period after injection, the efflux of ^{111}In radioactivity from organs is assumed to be negligible, because the degradation products of ^{111}In-labeled ligands using DTPA anhydride cannot easily pass through biologic membranes. This assumption was confirmed by the finding that ^{111}In was not detectable in the urine throughout the 120-minute period. At appropriate intervals after the injection, blood was collected from the vena cava under ether anesthesia and plasma was obtained by centrifugation (3000*g*, 10 minutes). The liver, kidney, spleen and lung were excised, rinsed with saline, and weighed. The radioactivity of each sample was measured in a well-type NaI scintillation counter (ARC-500; Hitachi Aloka Medical, Ltd., Tokyo, Japan).

Preparation of Bromobimane-Labeled SH-Man-HSA. A solution of 75 μM bromobimane in 0.1 M KPB was added to a solution of 100 μM SH-Man-HSA in 0.1 M KPB, followed by incubation for 2 hours at 4°C. The resulting solution was purified using a Pharmacia Bio-Gel PD-10 column (GE Healthcare, Little Chalfont Bucks, UK) and concentrated by Vivaspin (Sartorius Stedim Biotech S.A., Aubagne, France).

Evaluation of $CD68^+/CD206^+$ KC Distribution of SH-Man-HSA. The prepared bromobimane-labeled SH-Man-HSA (20.0 μmol SH/kg) was injected into the tail vein of mice. Mannan (6.0 mg/mouse) was injected intravenously 30 minutes before the bromobimane-labeled SH-Man-HSA administration. At 1 and 12 hours after the administration of bromobimane-labeled SH-Man-HSA, the liver was removed, covered with optimal cutting temperature compound, and frozen at −80°C. Fresh-frozen sections (4-μm thickness) of the liver were cut on a cryostat (CM3000II; Leica, Wetzlar, Germany), collected on slides, and immediately dried. The sections were fixed with phosphate-buffered 4% paraformaldehyde and washed. After incubation with 1% Block Ace (DS Pharma Biomedical, Osaka, Japan) for 10 minutes, the slides were incubated overnight with anti-HSA (Bethyl Laboratories, Inc., Montgomery, TX), CD68 (FA-11; BioLegend, San Diego, CA), and CD206 (C068C2; BioLegend) antibodies diluted 100, 100, or 200 times, respectively. After the reaction, the slide was observed using a microscope (BZ-8000; Keyence, Osaka, Japan).

Effect of SH-Man-HSA on Survival Rate of Lethal Con-A–Treated Mice. A lethal Con-A–treated mouse model was produced using C57BL/6 mice that were intravenously injected with Con-A (1.0 mg/mouse). The same SH content (20.0 μmol SH/kg) of SH-Man-HSA and NAC was administered intravenously just prior to the Con-A injection.

Hepatoprotective Effect of SH-Man-HSA on Con-A– or APAP-Treated Mice. Con-A– and APAP-induced liver injury mouse model was produced as previously reported (Ayoub et al., 2004; Nakashima et al., 2008; Saito et al., 2010). The animal experiment protocol is shown in Supplemental Figs. 4 and 5. Alanine aminotransferase (ALT) and aspartate aminotransferase (AST) activity levels were determined using a transaminase C2 test kit from Wako Chemicals (Saitama, Japan). In case of Con-A, the mice received 0.25 mg of Con-A intravenously (Sigma-Aldrich, St. Louis, MO). Just prior to Con-A injection, 5.0, 10.0, and 20.0 μmol SH/kg of SH-Man-HSA and 20.0 μmol SH/kg of NAC were administered intravenously to the mice. Likewise, SH-HSA (20.0 μmol SH/kg) or Man-HSA (2.66 μmol SH/kg) was administered intravenously. In case of APAP, the mice received 300 mg/kg of APAP intraperitoneally (Sigma-Aldrich). The same SH content (20.0 μmol SH/kg) of SH-Man-HSA and NAC was administered intravenously to the mice just prior to APAP injection. Furthermore, we administered SH-Man-HSA or NAC (intravenously) at 2 and 4 hours after the injection of Con-A or APAP. To inhibit the KC, especially $CD68^+$ cells, 200 μg of $GdCl_3$ was administered (Sigma-Aldrich) intravenously via the caudal vein 24 hours before Con-A or APAP injection. All mice were sacrificed 12 hours after Con-A or APAP injection.

Histologic Examination of Liver Tissues. Twelve hours after Con-A or APAP injection, the whole liver was removed. For the histologic analyses, the liver tissues were fixed in 10% neutral-buffered formalin (Wako Pure Chemical Industries, Osaka, Japan), embedded in paraffin (Sakura Finetek Japan, Tokyo, Japan), and sectioned at a 4-μm thickness. The liver sections were subjected to hematoxylin and eosin staining for morphologic analysis, terminal deoxynucleotidyl transferase dUTP nick-end labeling (TUNEL) staining for cell apoptosis, and immunohistochemistry for 8-OHdG (8-hydroxy-2′-deoxyguanosine) [15A3] (Santa Cruz Biotechnology, Dallas, TX) and nitrotyrosine (NO_2-Tyr) (Millipore, Billerica, MA). All assays were performed in triplicate. For TUNEL staining, sections were stained using the In Situ Cell Death Detection Kit, Fluorescein (Roche, Basel, Switzerland), according to the manufacturer's protocol for paraffin-embedded sections. For the immunohistochemistry of 8-OHdG and NO_2-Tyr, first, antigen retrieval was performed by means of an immunosaver (Nisshin EM Corporation, Tokyo, Japan). T-TB solution containing 50 mM Tris-HCl (pH 7.4) and 0.1% Tween-20 was then used to solubilize the liver slices, followed by blocking with Block Ace (Dainippon Pharmaceutics, Osaka, Japan) at room temperature for 10 minutes. Next, reaction with the primary antibody was carried out overnight at a temperature below 4°C. In addition, the primary antibody against 8-OHdG or NO_2-Tyr was diluted with 0.5% bovine serum albumin in PBS 50 times before use. The liver slices were then washed with T-TB solution, followed by reaction with the secondary antibody at room temperature for 1.5 hours. For 8-OHdG immunostaining, Alexa Fluor 488 goat anti-mouse IgG (H+L) (Invitrogen, Tokyo, Japan) and for NO_2-Tyr immunostaining, Alexa Fluor 546 goat anti-mouse IgG (H+L) (Invitrogen/Life Technologies) were diluted with 0.5% bovine serum albumin in PBS 200 times before use. After the reaction, the slide was observed under a microscope (BZ-8000; Keyence).

Quantification of Liver SH and GSH Levels. Tissue homogenates were prepared by homogenizing the tissues with 5% (w/v) sulfosalicylic acid. The homogenates were then centrifuged at 10,000*g* for 10 minutes at 4°C. SH levels were determined according to the DTNB method. Reduced and oxidized glutathione levels in the livers were determined using a reduced/oxidized GSH ratio (GSH/GSSG) quantification kit (Dojinkagaku, Kumamoto, Japan).

Determination of ROS in Liver Using EPR. The in vivo EPR analysis was performed as described previously with some modifications (Sato et al., 2002). The EPR spectra of POBN spin adducts of lipid peroxide radical LOO· were determined at 4 hours after Con-A or APAP injection. POBN (1.0 g/kg) was injected intraperitoneally at 30 minutes before the mice were sacrificed. The livers were homogenized in 1 ml of saline on an ice bath. The homogenates were added in 2 ml of 2:1 chloroform/methanol, shaken, then centrifuged at 2800 rpm for 10 minutes. The chloroform layer was isolated. After evaporating the sample by bubbling with N_2 in a vial, the sample was resuspended in organic solvent (200 μl of chloroform/methanol). EPR spectra were immediately recorded at room temperature in a JES-TE200 spectrometer (JEOL, Tokyo, Japan) under the following conditions: modulation frequency, 100 kHz; microwave frequency, 9.43 GHz; microwave power, 40 mW; scanning field, 333.5 mT; sweep time, 2 minutes; field modulation width, 0.25 mT; receiver gain, 630; and time count, 0.3 seconds. Every buffer and solution of the reaction mixture used for EPR measurement were treated with Chelex 100 resin (Bio-Rad Laboratories, Hercules, CA) before use to remove metals.

Isolation of Hepatic Mononuclear Cells and Flow Cytometry. Mononuclear cells were prepared as described previously (Dobashi et al., 1999). Liver specimens were minced with scissors. After adding a 0.25% collagenase solution, the specimens were shaken for 20 minutes in a 37°C constant-temperature bath. The liver specimen was then filtered through a nylon mesh (108 μm). After mixing in 33% Percoll solution containing heparin (1%), the sample was centrifuged for 20 minutes at 500*g* at room temperature. After removing the supernatant, the pellet was resuspended in a red blood cell lysis solution and then was washed twice in RPMI 1640 with 10% fetal bovine serum. For identification of KC, mononuclear cells were stained by phycoerythrin Cy5-conjugated anti-F4/80 antibody (eBioscience, San Diego, CA). For the detection of intracellular ROS, CM-H_2DCFDA (Invitrogen, Carlsbad, CA), an ROS-sensitive fluorescent dye used as probe. Also, for the detection of macrophage polarization status, anti–inducible NO synthase (Santa Cruz Biotechnology, Santa Cruz, CA) and CD206 (C068C2; BioLegend) antibody were used. $F4/80^+$ KC were isolated by positive selection according to the manufacturer's protocol (MACS isolation system; Miltenyi Biotec, Auburn, CA). Flow cytometry was performed using a FACSCalibur (BD Biosciences, San Jose, CA).

Quantification of TNF and Interferon-γ Levels. TNF and interferon (IFN)-γ levels in plasma at 1 and 12 hours, respectively, after Con-A (0.25 mg/mouse) injection were measured by enzyme-linked immunosorbent assay, following the manufacturer's recommended protocol.

Statistical Analysis. All data are expressed as mean ± S.E. The means for groups were compared by analysis of variance followed by Tukey's multiple comparison and Student's *t* test. The survival rates were compared using Kaplan-Meier survival curves and the log-rank test. A probability value of $P < 0.05$ was considered significant.

Results

Radical-Scavenging Activity of SH-Man-HSA. We developed SH-Man-HSA (7.5 mol SH/mol of Man-HSA) using 2-iminothiolane (Supplemental Fig. 2A) and its radical-scavenging activity against ·OH radicals was evaluated using an EPR method. Figure 1A shows the EPR signal derived from ·OH radicals in the absence (control) and presence of HSA, Man-HSA, and SH-Man-HSA. In the presence of HSA and Man-HSA, the signal intensity decreased to 40 and 50% of the control, respectively, whereas SH-Man-HSA inhibited the intensity by nearly 80%, indicating that SH-Man-HSA has more potent ROS-scavenging activity than HSA and Man-HSA (Fig. 1B).

Pharmacokinetic Analysis of SH-Man-HSA. A pharmacokinetic analysis of the SH-Man-HSA showed that 50% of the administered dose was distributed to the liver within about 20 minutes, similar to previously reported findings for

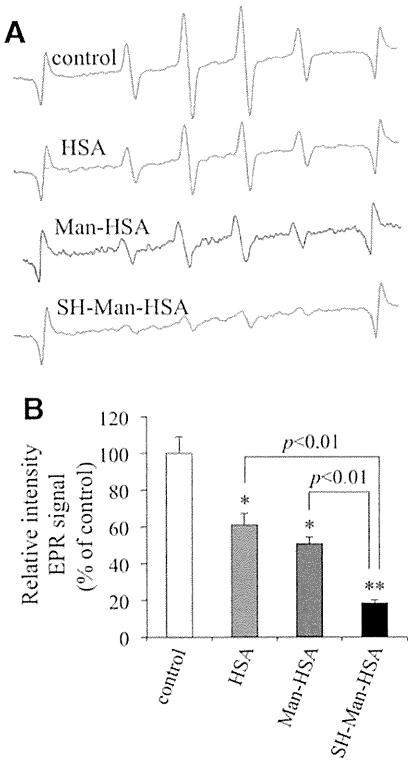

Fig. 1. Radical-scavenging activity of the SH-Man-HSA. (A) EPR spectra of ·OH and (B) the quantification of signal intensity were determined using an EPR method. The reaction solution contained 100 μM DTPA, 9 mM DMPO, and 500 μM H_2O_2 in the absence or presence of 75 μM HSA, Man-HSA, or SH-Man-HSA in PBS (pH 7.4). Each value represents the mean ± S.E. (n = 3). *P < 0.05; **P < 0.01 compared with control.

Man-HSA (Fig. 2A) (Hirata et al., 2010). Furthermore, the hepatic distribution of SH-Man-HSA was investigated by means of a fluorescence-imaging technique. In this procedure, the SHs of SH-Man-HSA were completely modified by the treatment with bromobimane. Liver sections were observed at 1 hour after the administration of bromobimane-labeled SH-Man-HSA (20.0 μmol SH/kg), and modified SH groups were detected with a fluorescence probe in the form of a blue emission. As shown in Fig. 2B, substantial fluorescence was observed in the liver sections, especially near the sinusoidal regions. Such a fluorescence was largely inhibited by the preadministration of a two times higher dose of mannan, a typical substrate for CD206, suggesting the importance of this receptor for distributing SH-Man-HSA to the liver.

At the region near the sinusoid, there are several cells that express CD206, such as KC, endothelial cells, and dendritic cells (Kogelberg et al., 2007). Our previous study revealed that Man-HSA was preferentially distributed to KC, but not to endothelial cells (Hirata et al., 2010). It has been demonstrated that the C-type lectin–like domain binds complex carbohydrates in which the chains are terminated with mannose, such as Man(n)GlcNAc2 (n, numbers of mannose residues). For instance, the carbohydrate-recognition domain of Dectin-2 is a C-type lectin with a very high affinity for high-mannose structures, especially structures that contain more than seven mannose residues, and its specificity is enhanced with an increase in the number of mannose residues (McGreal et al., 2006). Interestingly, Dectin-2 expression was predominantly restricted to CD206-positive macrophages (Sun et al., 2013). Because SH-Man-HSA possesses an oligosaccharide chain with Man(12)GlcNAc2, it would be expected to be preferentially recognized by Dectin-2 on KC that express CD206, but not endothelial cells.

Evaluation of $CD68^+/CD206^+$ KC Distribution of SH-Man-HSA. To further characterize the distribution of SH-Man-HSA to KC subtype, liver sections were subjected to immunostaining with anti-HSA, CD68, and CD206 antibodies. The anti-HSA antibody used in this study did not crossreact with the mouse species. At 1 hour after the administration of bromobimane-labeled SH-Man-HSA, the fluorescence derived from bromobimane (blue) was merged with both the fluorescence of the anti-HSA antibody (red) and the anti-CD68 antibody (green) as shown by white spots in the inset image (Fig. 3A). Similar white spots that had merged with the fluorescence of bromobimane, the anti-HSA antibody, and the anti-CD206 antibody (green) were also observed (Fig. 3B). These data indicate that SH-Man-HSA was efficiently distributed to $CD68^+/CD206^+$ KC within 1 hour after the administration of bromobimane-labeled SH-Man-HSA depending on its unique oligosaccharide moiety. However, the fluorescence of bromobimane did not become merged with both the fluorescences of the anti-HSA antibody and the anti-CD68 antibody at 12 hours after the administration of bromobimane-labeled SH-Man-HSA (Fig. 3C, right panel), suggesting that SH-Man-HSA is susceptible to lysosomal degradation in $CD68^+/CD206^+$ KC, and that the majority of the SH moieties were liberated from SH-Man-HSA and moved to the outside of $CD68^+/CD206^+$ KC.

Hepatoprotective Effect of SH-Man-HSA on Con-A–Treated Mice. To examine the effect of SH-Man-HSA on liver injury, we used a Con-A–induced hepatitis model, because it has been widely used as a model for liver injury, such as autoimmune and viral types. As shown in Fig. 4A, all of the saline-treated mice died within 28 hours after a lethal dose (1.0 mg/mouse i.v.) of Con-A, whereas 20% of the NAC (20.0 μmol SH/kg)-treated mouse group survived. Interestingly, the administration of SH-Man-HSA (20.0 μmol SH/kg) resulted in a significant increase in survival rate, with 70% of the mice being alive at 60 hours after the Con-A injection.

The hepatoprotective effects of SH-Man-HSA were evaluated to monitor ALT and AST levels at 12 hours after the injection of a low dose (0.25 mg/mouse i.v.) of Con-A because the plasma ALT and AST levels were at a maximum at 12 hours post Con-A injection (Supplemental Fig. 6). SH-Man-HSA suppressed the elevation of plasma ALT and AST levels that had been induced by Con-A in a dose-dependent manner. In particular, 20.0 μmol SH/kg of SH-Man-HSA inhibited the elevation of ALT and AST plasma levels by 98 and 99% for Con-A–treated mice (Fig. 4B). Therefore, 20.0 μmol SH/kg of SH-Man-HSA was adopted in the subsequent experiments (Supplemental Fig. 3).

The elevation in levels of plasma ALT and AST in Con-A–treated mice was also suppressed by 20.0 μmol SH/kg of NAC, but the effect was much less than by SH-Man-HSA. On the other hand, pretreatment with $GdCl_3$ at 24 hours before the Con-A injection resulted in a hepatoprotective effect that was equivalent to 20.0 μmol SH/kg of SH-Man-HSA (Fig. 4B).

Histologic examinations of liver tissue in Con-A–induced hepatitis were also performed with H&E and TUNEL staining (Fig. 4C). H&E staining of liver sections showed evidence of massive necrosis within the liver lobules in the

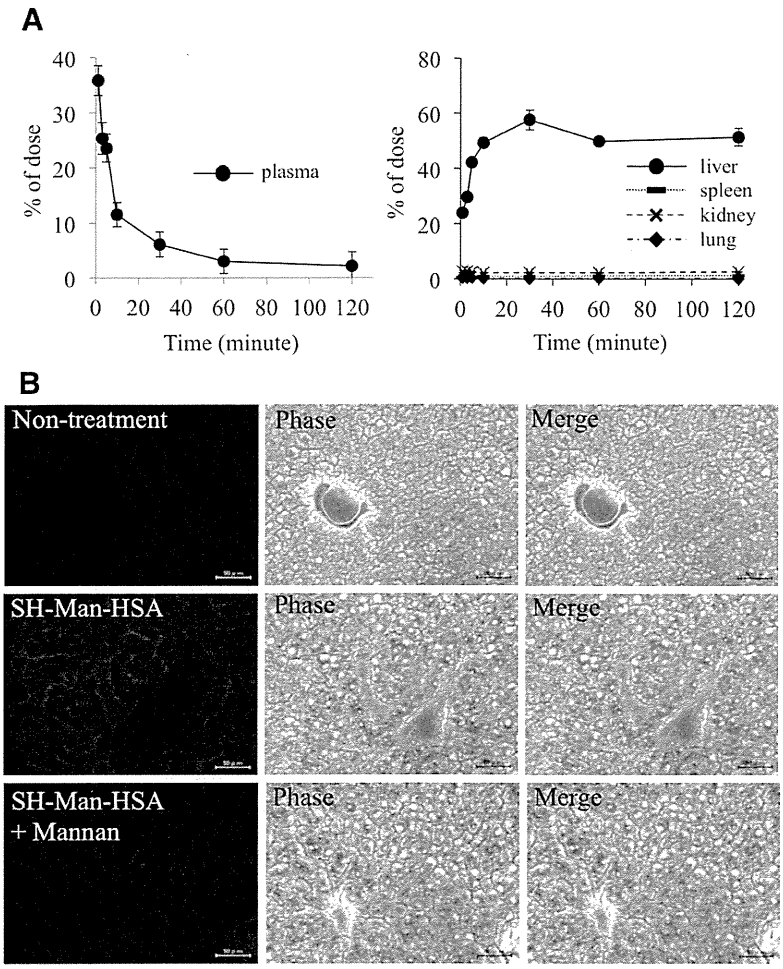

Fig. 2. Pharmacokinetic analysis of the SH-Man-HSA. (A) Plasma concentration curve and organ distribution of SH-Man-HSA after 10.0 nmol SH/kg of ^{111}In-labeled SH-Man-HSA was injected in tail vein of mice. Each value represents the mean ± S.E. (n = 3). (B) Furthermore, SH-Man-HSA distribution in the liver was observed in liver section using fluorescence image technique at 1 hour after the administration of bromobimane-labeled SH-Man-HSA (20.0 μmol SH/kg; original magnification, 400×). Thirty minutes before the administration of bromobimane-labeled SH-Man-HSA, 6.0 mg/mouse of mannan was administered.

saline treatment group of the Con-A–challenged mice. Similar results were obtained for TUNEL staining. In the saline treatment groups, a number of TUNEL-positive hepatocytes were observed for the Con-A–induced model, whereas no evidence for such positive cells was found in the case of the SH-Man-HSA and $GdCl_3$ treatment groups. NAC also reduced TUNEL-positive cells, but to a lesser extent compared with SH-Man-HSA.

The contribution of each functional component was examined in the Con-A–induced model using two HSA derivatives, namely, Man-HSA, which contains mannose residues but no additional SH groups, and SH-HSA, which contains additional SH moieties, but no mannose residues. As shown in Fig. 4D, Man-HSA (2.66 μmol SH/kg) and SH-HSA (20.0 μmol SH/kg) significantly attenuated the Con-A–induced elevation in plasma ALT and AST levels. The extent of attenuation was in the following order: Man-HSA < SH-HSA < SH-Man-HSA.

Effect of SH-Man-HSA on Hepatic SH Level and Oxidative Stress Induced by Con-A. SH levels in liver homogenates were determined 12 hours after the injection of Con-A (Fig. 5A) to evaluate the efficacy of SH delivery to the liver by SH-Man-HSA and NAC, both of which had the same SH content (20.0 μmol SH/kg). The SH level of the saline-treated groups was decreased by Con-A injection, and it recovered in the following treatment order: NAC < $GdCl_3$ < SH-Man-HSA. Furthermore, as shown in Fig. 5B, SH-Man-HSA suppressed the decrease in GSH/GSSG, indicating that SH-Man-HSA is superior to NAC in terms of delivering SH to the liver.

The effects of SH-Man-HSA or NAC on Con-A–induced free radical formation in the liver were directly monitored in vivo using an EPR technique (Fig. 5C), in which LOO· levels were determined in a liver homogenate. Radical production increased in a time-dependent manner, reaching a maximum at 4 or 5 hours after the Con-A injection (Supplemental Fig. 7). As shown in Fig. 5D, more than 80% of the EPR signal induced by the Con-A challenges was inhibited by both SH-Man-HSA and $GdCl_3$, whereas less than 40% of the signal intensity was decreased by NAC at 4 hours after the Con-A injection. Similar antioxidative effects of SH-Man-HSA were also confirmed by immunostaining of 8-OHdG and NO_2-Tyr, markers for oxidative and nitrative stress, respectively, in the liver (Fig. 5E). In addition, Con-A markedly increased the fluorescence intensity of ROS derived from F4/80$^+$/ROS$^+$–detecting probe (168 ± 27), whereas it was significantly inhibited by both SH-Man-HSA (57 ± 6) and $GdCl_3$ (70 ± 5) (Fig. 5F). Such similar inhibitions of ROS production in F4/80$^+$/ROS$^+$ cells between SH-Man-HSA and $GdCl_3$ could reflect comparable action against Con-A–induced hepatic damage.

On the other hand, the possibility that the ROS-scavenging activity of SH-Man-HSA might be mediated via the inhibition of TNF or IFN-γ that is closely associated with Con-A–induced

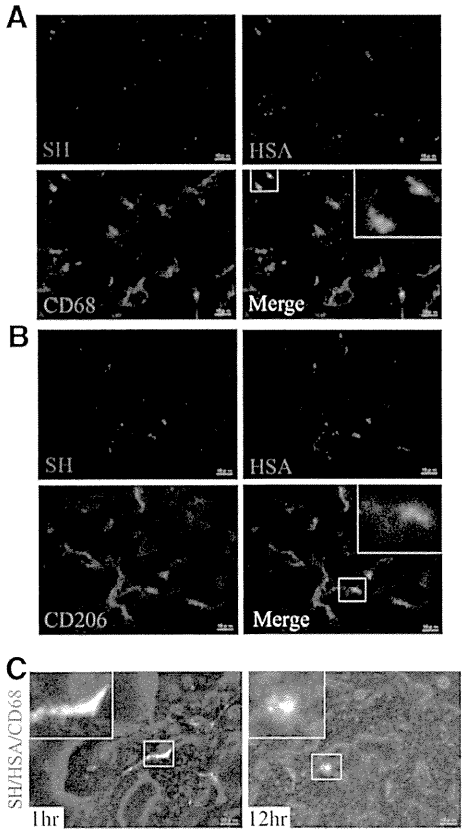

Fig. 3. Evaluation of $CD68^+/CD206^+$ KC distribution of SH-Man-HSA. The prepared bromobimane-labeled SH-Man-HSA (3.6 mg/mouse) was injected into the tail vein of mice. At 1 and 12 hours after the administration of bromobimane-labeled SH-Man-HSA, the liver was removed, covered with optimal cutting temperature compound and frozen at −80°C. Fresh-frozen sections (4-μm thickness) of the liver were cut on a cryostat, collected on slides, and immediately dried. The sections were fixed with phosphate-buffered 4% paraformaldehyde and then washed. After incubation with 1% Block Ace for 10 minutes, the slides were incubated overnight with anti-HSA, CD68, and CD206 antibody diluted 100, 100, or 200 times, respectively. (A and B) SH-Man-HSA distribution in subtypes of KC was observed in liver at 1 hour after the administration of bromobimane-labeled SH-Man-HSA (3.6 mg/mouse) (original magnification, 1200×). (C) Fluorescence images of anti-HSA antibody and bromobimane in $CD68^+$ KC at 1 (left) or 12 hours (right) after the administration of bromobimane-labeled SH-Man-HSA (3.6 mg/mouse) (original magnification, 1200×). The fluorescence of bromobimane (blue) and the anti-HSA antibody (red) merged cells were a purple color. The fluorescence of the anti-HSA antibody and either anti-CD68 antibody or anti-CD206 antibody (green) merged cells were a yellow color. The fluorescences of bromobimane, anti-HSA antibody, and either anti-CD68 antibody or anti-CD206 antibody merged cells were a white color. Insets: enlarged image of white square–marked typical section.

hepatic damage cannot be completely excluded. However, SH-Man-HSA did not decrease to the levels of TNF or IFN-γ (Fig. 5G).

Hepatoprotective Effect of SH-Man-HSA on APAP-Treated Mice. The hepatoprotective effect of SH-Man-HSA was also examined against an APAP-induced hepatic injury model that was prepared by an intraperitoneal injection of 300 mg/kg of APAP (Fig. 6). As in the case of Con-A–induced hepatitis, equal SH contents (20.0 μmol SH/kg) of SH-Man-HSA or NAC were administered (intravenously) just before APAP injection, and the plasma ALT and AST levels were measured at 12 hours after APAP injection (Supplemental Fig. 8). As a result, SH-Man-HSA largely inhibited APAP-induced elevation of plasma ALT and AST levels by 96 and 94%, respectively. NAC also significantly suppressed the plasma ALT and AST levels by 61 and 57%, respectively, but this effect was much less than that of SH-Man-HSA. Pretreatment with $GdCl_3$ showed hepatoprotective effects similar to SH-Man-HSA administration (Fig. 6A). This is consistent with the previous finding that KC play an important role in the development of APAP-induced hepatic injury.

H&E staining of liver sections indicated that the APAP-induced massive necrosis within the centralobular region of the livers, as evidenced by the loss of basophilic staining, vacuolization, cell swelling, and karyolysis around the centrilobular veins, as previously reported (Fig. 6B, upper panel). However, liver sections from SH-Man-HSA administration showed little damage, and a nearly normal morphology was preserved. Similar results were also obtained for a $GdCl_3$ pretreatment. H&E staining of tissue from the NAC administration group showed some improvement in the integrity of liver sections against APAP-induced hepatotoxicity, but its efficacy was less than that of SH-Man-HSA and $GdCl_3$. Similar results were obtained for TUNEL staining (Fig. 6B, lower panel). In the saline treatment group, a number of TUNEL-positive hepatocytes were observed, whereas such positive cells could not be found after SH-Man-HSA and $GdCl_3$ administration groups. NAC also reduced TUNEL-positive cells, but to a lesser extent compared with SH-Man-HSA.

Effect of SH-Man-HSA on Hepatic SH Level and Oxidative Stress Induced by APAP. Figure 7A shows SH levels in liver homogenates 12 hours after the injection of mice with APAP. The SH levels in liver were significantly decreased as a result of the APAP injection, but the level was completely recovered by the subsequent SH-Man-HSA administration or a $GaCl_3$ pretreatment. In contrast, the administration of NAC was ineffective in recovering APAP-induced SH depletion in the liver. Furthermore, as shown in Fig. 7B, SH-Man-HSA suppressed the decrease in GSH/GSSG, indicating that SH-Man-HSA is superior to NAC in delivering SH to the liver.

Figure 7, C and D, shows the effect of SH-Man-HSA on the lipid peroxide radical in liver homogenate after APAP injection to mice. As observed in the Con-A–induced hepatopathy model, a remarkable EPR signal was detected at 4 hours after APAP injection (Supplemental Fig. 9). This EPR signal was significantly suppressed by the SH-Man-HSA or $GdCl_3$ pretreatment by approximately 70%, but NAC treatment only decreased the signal intensity by approximately 40%.

Previous findings revealed that oxidative and nitrative toxicity in liver induced by APAP included lipid peroxidation and protein nitration (Michael et al., 1999). As shown in Fig. 7E, our immunostaining data against 8-OHdG and NO_2-Tyr demonstrated that SH-Man-HSA administration effectively inhibited the accumulation of those oxidized products in the liver induced by APAP, whereas NAC was less effective in inhibiting the accumulation of those oxidative stress markers. Furthermore, to clarify the antioxidative activity of SH-Man-HSA in KC of APAP-induced hepatic injury mice, the $F4/80^+/ROS^+$ KC population was estimated at 4 hours after APAP injection (300 mg/kg i.p.) by flow cytometry (Fig. 7F). $F4/80^+/ROS^+$ KC increased following the APAP injection, whereas it was decreased by SH-Man-HSA administration. Pretreatment with $GdCl_3$ also decreased the content of $F4/80^+/ROS^+$ KC, to the lesser extent.

Effect of Postadministration of SH-Man-HSA on Con-A– or APAP-Treated Mice. To investigate the potential of

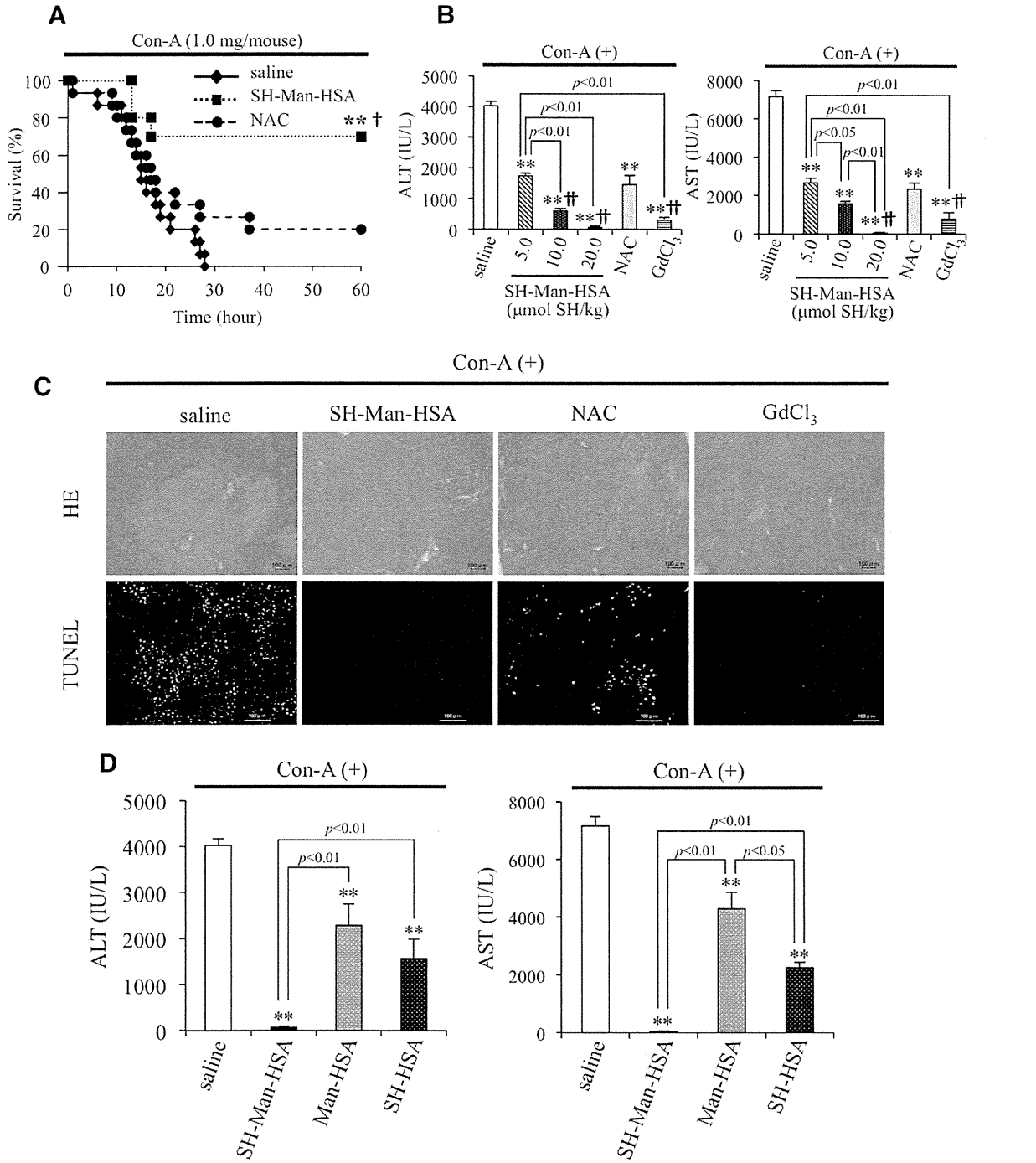

Fig. 4. Survival and hepatoprotective effect of SH-Man-HSA on lethal and low dose of Con-A–treated mice. (A) Identical SH contents (20.0 μmol SH/kg) of SH-Man-HSA and NAC were administered intravenously just prior to lethal dose of Con-A (1.0 mg/mouse i.v.) injection (n = 10–15). $^{**}P < 0.01$ compared with saline; $^{\dagger}P < 0.05$ compared with NAC. (B) Just prior to low dose of Con-A (0.25 mg/mouse), 5.0, 10.0, and 20.0 μmol SH/kg SH-Man-HSA and 20.0 μmol SH/kg NAC were administered intravenously, and $GdCl_3$ (200 μg/mouse) was administered intravenously at 24 hours prior to the Con-A injection. Plasma ALT and AST levels were determined at 12 hours after Con-A injection. Each value represents the mean ± S.E. (n = 4–6). $^{**}P < 0.01$ compared with saline; $^{\dagger\dagger}P < 0.01$ compared with NAC. (C) H&E and TUNEL staining (original magnification, 100× and 200×, respectively) of mice liver were performed at 12 hours after the Con-A injection. (D) Just prior to the Con-A injection, 2.66 μmol SH/kg of Man-HSA or 20.0 μmol SH/kg of SH-HSA was administered intravenously. Each value represents the mean ± S.E. (n = 3). $^{**}P < 0.01$ compared with saline.

SH-Man-HSA as a rescue therapy after Con-A or APAP challenges, equal SH contents (20.0 μmol SH/kg) of SH-Man-HSA or NAC were administered 2 and 4 hours following an injection of Con-A (intravenously) or APAP (intraperitoneally).

As shown in Fig. 8, the administration of SH-Man-HSA 2 hours after Con-A or APAP injection largely inhibited the elevation in ALT and AST levels. In addition, even 4 hours after the Con-A or APAP injection, SH-Man-HSA significantly

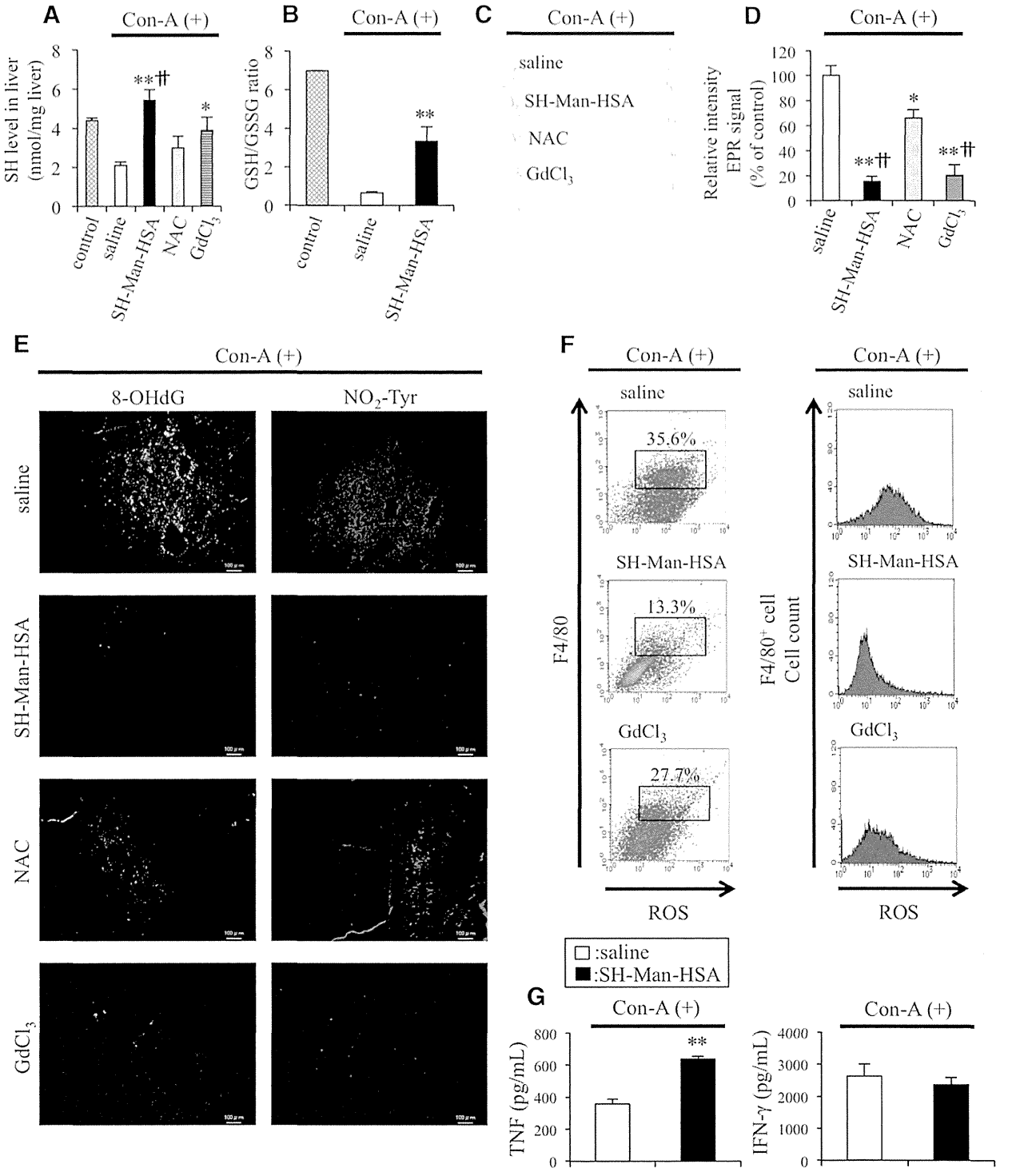

Fig. 5. Effect of SH-Man-HSA on hepatic SH level and oxidative stress induced by Con-A. Identical SH contents (20.0 μmol SH/kg) of SH-Man-HSA and NAC were administered intravenously just prior to Con-A (0.25 mg/mouse) injection, and $GdCl_3$ (200 μg/mouse) was administered intravenously at 24 hours before Con-A. Livers were excised and homogenized at 12 hours after the Con-A injection. After deproteination of homogenized liver samples, (A) SH levels and (B) GSH/GSSG ratios in the supernatant were measured by the DTNB method. Each value represents the mean ± S.E. (n = 4–6). *$P < 0.05$; **$P < 0.01$ compared with saline; $^{\dagger\dagger}P < 0.01$ compared with NAC. (C) EPR spectra of POBN spin adducts of lipid peroxide radical *LOO* and (D) the quantification of signal intensity was done at 4 hours after Con-A injection. POBN (1.0 g/kg) was administered intraperitoneally at 30 minutes before mice were sacrificed. Each value represents the mean ± S.E. (n = 3–4). *$P < 0.05$; **$P < 0.01$ compared with saline; $^{\dagger\dagger}P < 0.01$ compared with NAC. (E) Immunostaining of 8-OHdG and NO_2-Tyr in liver tissue was performed at 12 hours after the Con-A injection (original magnification, 100×). (F) Mononuclear cells were obtained from liver at 4 hours after Con-A injection. Gated $F4/80^+/ROS^+$ areas and ROS production derived from KC were analyzed by flow cytometry. (G) TNF and IFN-γ levels in plasma at 1 and 12 hours, respectively, after Con-A (0.25 mg/mouse) injection with or without SH-Man-HSA (20.0 μmol SH/kg) administration (n = 4). **$P < 0.01$ compared with saline; Student's t test.

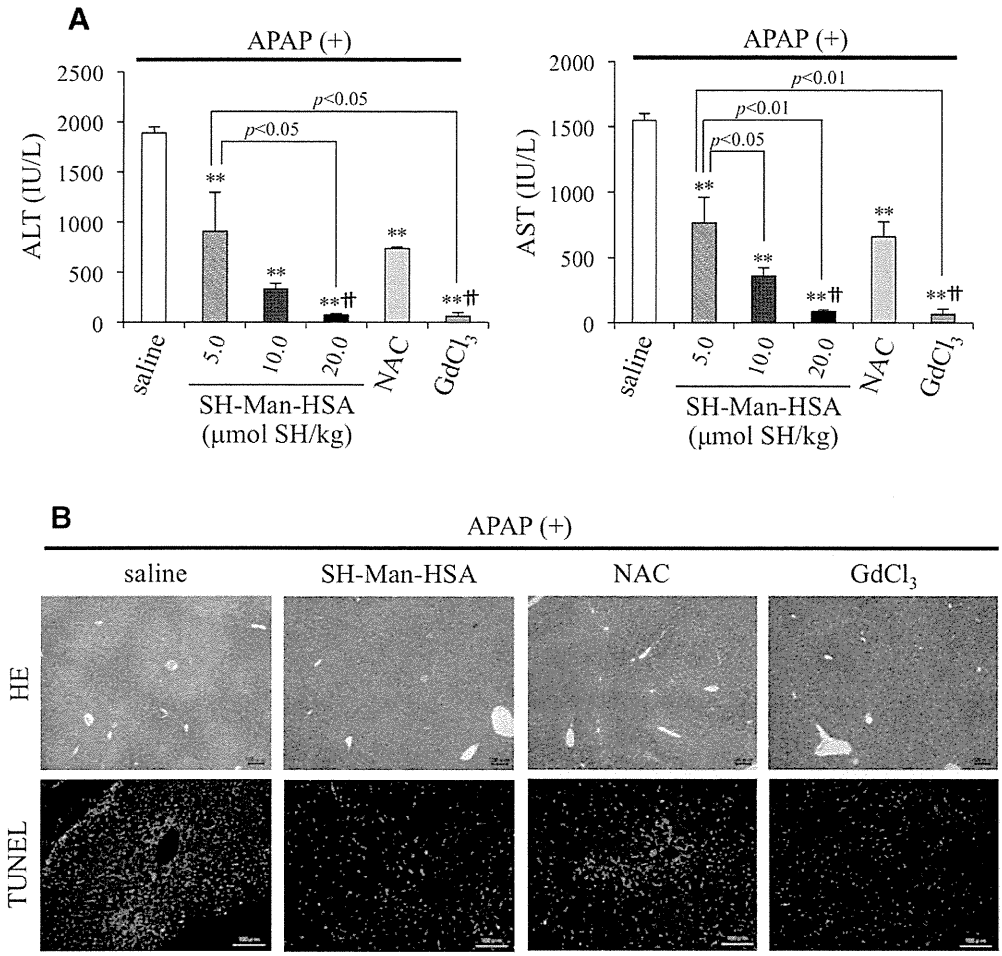

Fig. 6. Hepatoprotective effect of SH-Man-HSA on APAP-treated mice. Just prior to APAP injection (300 mg/kg) 5.0, 10.0, and 20.0 μmol SH/kg SH-Man-HSA and 20.0 μmol SH/kg NAC were administered intravenously, and $GdCl_3$ (200 μg/mouse) was administered intravenously at 24 hours before APAP injection. (A) Plasma ALT and AST levels were determined at 12 hours after APAP injection. Each value represents the mean ± S.E. (n = 4–6). $^{**}P < 0.01$ compared with saline; $^{\dagger\dagger}P < 0.01$ compared with NAC. (B) H&E and TUNEL staining (original magnification, 100× and 200×, respectively) of mouse liver tissue were performed at 12 hours after APAP injection.

reduced the elevation of ALT and AST. In contrast, the administration of NAC 2 or 4 hours later did not exhibit sufficient hepatoprotective action in either of the models.

A previous study reported that the administration of a high dose (650 μmol SH/kg) of NAC (intravenously) at 1.5 hours after an APAP injection (300 mg/kg i.p.) exhibited a significant hepatoprotective action (Saito et al., 2010). Thus, the effect of 650 μmol SH/kg of NAC on APAP-induced hepatic injury at 2 or 4 hours after an APAP injection (300 mg/kg i.p.) was also examined. At 2 hours following the APAP injection, a high dose of NAC showed a greater suppressive effect on ALT (84%) and AST (80%) elevation than a low dose (20.0 μmol SH/kg), as shown in Fig. 8B. However, a high dose of NAC showed only a small inhibitory effect against ALT and AST elevations at 4 hours after the APAP injection. These data indicate that SH-Man-HSA was a more effective agent for treating these experimental acute liver injuries compared with NAC.

To confirm whether the hepatoprotective action derived from the postadministration of SH-Man-HSA resulted from the inhibition of hepatic oxidative stress as well as the pretreatment, we carried out histopathological and oxidative stress analyses after a post-treatment with SH-Man-HSA to Con-A– and APAP-induced hepatopathy models. The liver sections of H&E and the 8-OHdG staining of the SH-Man-HSA treatment at 2 hours after the Con-A and APAP injections clearly showed that SH-Man-HSA effectively inhibited liver damage and hepatic oxidative stress (Supplemental Fig. 10), confirming that, even though a post-treatment, SH-Man-HSA showed hepatoprotective action via the inhibition of hepatic oxidative stress similar to that observed for the pretreatment.

Discussion

The main goal of the present study was to design a system for delivering a nanoantioxidant containing SH groups to KC, especially $CD68^+/CD206^+$, using mannose as a recognition element for use as a rescue therapeutic agent in treating various acute liver injuries. HSA is a simple protein and contains no oligosaccharide chain structures. However, the insertion of a consensus sequence for an oligosaccharide chain into the albumin gene (D63N, A320T, D494N) results in a protein that contains an oligosaccharide chain, as in some reported genetic variants (Minchiotti et al., 2001). The pharmacokinetic properties and biologic activities of these glycosylated mutants of HSA

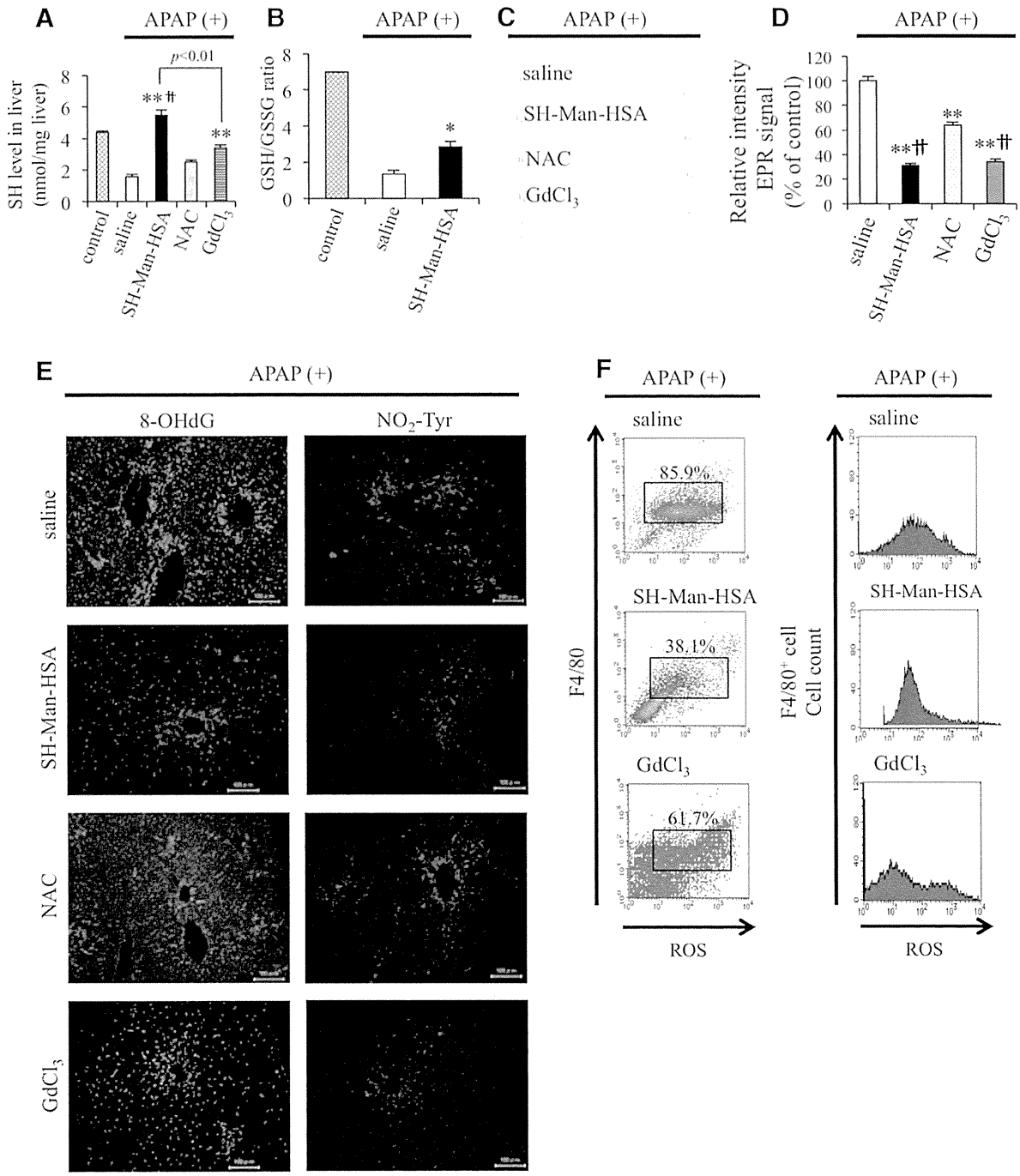

Fig. 7. Effect of SH-Man-HSA on hepatic SH level and oxidative stress induced by APAP. Identical SH contents (20.0 μmol SH/kg) of SH-Man-HSA and NAC were administered intravenously just prior to the APAP (300 mg/kg) injection, and $GdCl_3$ (200 μg/mouse) was administered intravenously just prior to the APAP injection. Livers were excised and homogenized at 12 hours after APAP injection. After deproteination of homogenized liver, (A) SH level and (B) GSH/GSSG ratio in supernatant was measured by DTNB method. Each value represents the mean ± S.E. (n = 4–6). *$P < 0.05$; **$P < 0.01$ compared with saline; $^{\dagger\dagger}P < 0.01$ compared with NAC. (C) EPR spectra of POBN spin adducts of lipid peroxide radical LOO· and (D) the quantification of signal intensity were determined at 4 hours after the APAP injection. POBN (1.0 g/kg) was administered intraperitoneally at 30 minutes before sacrifice of the mice. Each value represents the mean ± S.E. (n = 3–4). **$P < 0.01$ compared with saline; $^{\dagger\dagger}P < 0.01$ compared with NAC. Immunostaining of (E) 8-OHdG and NO_2-Tyr in liver tissue was performed at 12 hours after APAP injection (original magnification, 200×). (F) Hepatic mononuclear cells were obtained from liver at 4 hours after APAP injection. Gated $F4/80^+/ROS^+$ areas and ROS production derived from KC were analyzed by flow cytometry.

are similar to the wild-type molecule. Yeast expression systems were used to produce the Man-HSA because generally glycoproteins that are expressed in yeast possess high mannose-type glycan chains, which are different from those expressed by mammalian cells. We previously showed that Man-HSA is suitable for use as a drug delivery system carrier in targeting KC owing to its pharmacokinetic properties, which include its rapid and efficient distribution to the liver and the fact that it is selectively distributed to KC by CD206, unlike other chemically modified mannosylated carriers (Hirata et al.,

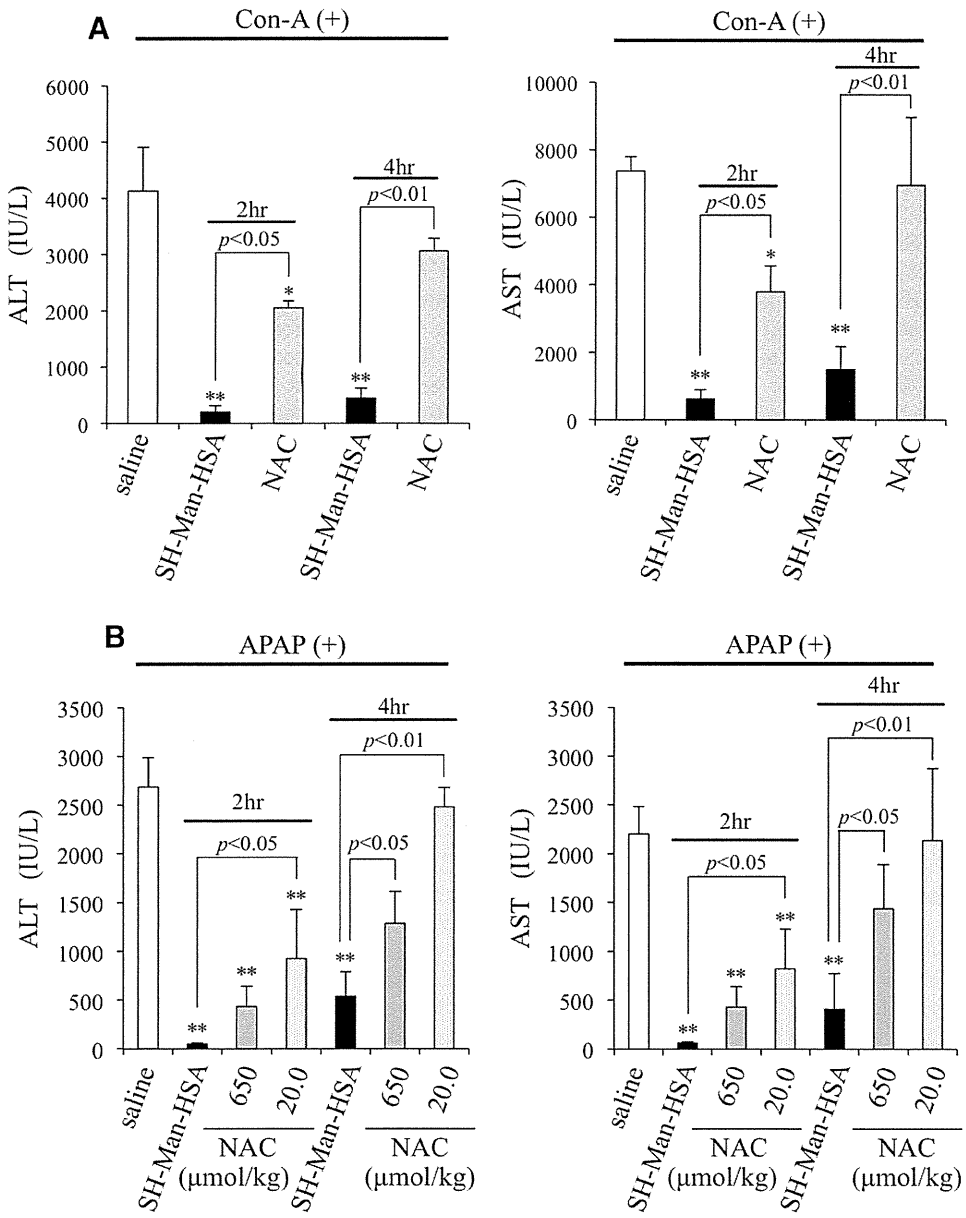

Fig. 8. Effect of postadministration of SH-Man-HSA on Con-A– or APAP-treated mice. Identical SH contents (20.0 μmol SH/kg) of SH-Man-HSA and NAC or high dose of NAC (650 μmol SH/kg) were intravenously administered at 2 or 4 hours after (A) Con-A (0.25 mg/mouse) or (B) APAP (300 mg/kg) injection. Plasma ALT and AST levels were determined at 12 hours after Con-A or APAP injection. Each value represents the mean ± S.E. (n = 3–5). *P < 0.05; **P < 0.01 compared with saline.

2010). The subsequent addition of an average of 7.5 mol SH groups to each Man-HSA molecule did not alter its unique hepatic distribution properties, and furthermore, the immunohistochemical evaluations reported here clearly showed that, among the KC subtypes, SH-Man-HSA is efficiently distributed to $CD68^+/CD206^+$ KC (Fig. 3). As far as we know, this is the first study to report on the development of a carrier for targeting $CD68^+/CD206^+$ KC. Thus, SH-Man-HSA meets the requirement for use as a $CD68^+/CD206^+$ KC directed nanoantioxidant because it confers more potent ROS-scavenging activity than HSA (Fig. 1).

Con-A– (Nakashima et al., 2008) and APAP-induced hepatitis (Ayoub et al., 2004; Saito et al., 2010) mouse models were used to evaluate the efficacy of SH-Man-HSA as a $CD68^+$ KC-directed antioxidant in the present study. The most frequent single cause of acute liver failure is an APAP overdose, accounting for 46% of the reported cases in the United States (Lee et al., 2008). In addition, the characteristics of an APAP-induced hepatitis mouse model of liver injury are similar to those for human patients on the basis of clinical observations and biochemical and histopathological data, and has been used in the past to identify potential therapeutic interventions. In fact, the present study demonstrated that the efficient delivery of SH to $CD68^+/CD206^+$ KC exhibited excellent hepatoprotective action against two models of acute hepatopathy. As mentioned in the introduction section, it is generally thought that ROS generated by $CD68^+$ KC play an important role in the initiation or progression of liver pathologic conditions. Our results provide more insights into involvement of $CD68^+/CD206^+$ KC in the development of acute liver injury. In addition, the present study also demonstrated that at an equal dose of SH (20.0 μmol SH/kg), SH-Man-HSA was superior to NAC in terms of improving the survival rate of Con-A–treated mice (Fig. 4A), and of alleviating liver damage in

Con-A– and APAP-induced hepatitis models as evidenced by the suppression of ALT and AST (Figs. 4B and 6A) and H&E staining (Figs. 4C and 6B). Because the hepatoprotective effect of Man-HSA and SH-HSA were not comparable to that of SH-Man-HSA (Fig. 4D), this suggests that both mannose residues and SH are essential for the therapeutic effect of SH-Man-HSA against a hepatic injury. The hepatoprotective effect observed for SH-Man-HSA was similar to that for a $GdCl_3$ pretreatment (Figs. 4B and 6A), indicating that SH-Man-HSA, when delivered to $CD68^+$ KC, could efficiently scavenge ROS generated in response to Con-A or APAP. In addition, excellent ROS-scavenging activity was evident for SH-Man-HSA, as evidenced by in vivo EPR, flow cytometry, and oxidative or nitrative stress markers (8-OHdG, NO_2-Tyr) (Figs. 5, C–F, and 7, C–F).

On the other hand, it is well known that Con-A activates T cells to produce IFN-γ via binding to T-cell receptors. IFN-γ, in turn, activates $CD68^+$ KC to produce TNF that interacts with the TNF receptor on the $CD68^+$ KC to produce ROS (Nakashima et al., 2008; Kinoshita et al., 2010). The possibility that the ROS-scavenging activity of SH-Man-HSA might be mediated via the inhibition of TNF or IFN-γ cannot be completely excluded. Interestingly, SH-Man-HSA levels did not decrease to the levels of these inflammatory factors. This result indicates that SH-Man-HSA attenuates Con-A–induced hepatopathy regardless of the levels of these inflammatory factors (Fig. 5G). Therefore, SH-Man-HSA exhibited its hepatoprotective effect, not by influencing TNF or IFN-γ production, but by suppressing ROS production produced by $CD68^+/CD206^+$ KC, which occurs downstream from the production of these cytokines. Similar results were reported for other antioxidants, such as edarabone and lecithinized superoxide dismutase, in Con-A–induced hepatitis (Nakashima et al., 2008).

There is a possibility that mannose residues or HSA molecules of SH-Man-HSA directly interact with the injected Con-A molecules, thus leading to suppression of the toxicity of Con-A. If this is correct, TNF and IFN-γ, which are involved in the development of Con-A–induced hepatopathy, should not be increased after the coadministration of Con-A and SH-Man-HSA. However, we found similar elevations of these inflammatory factors between Con-A injection and coadministration of SH-Man-HSA and Con-A, indicating that Con-A still preserved the potency that causes the induction of hepatic damage when SH-Man-HSA and Con-A were coadministrated. This clearly excludes the possibility that mannose residues or HSA of SH-Man-HSA directly inactivate the hepatic toxicity of Con-A. In fact, the postadministration of SH-Man-HSA also ameliorated the Con-A–induced liver injury via the mechanism similar to that of the pretreatment (Supplemental Fig. 10).

The role of ROS in APAP toxicity has been a subject of debate for decades and is not without its controversies (James et al., 2003). However, the pathologic role of ROS has not been fully understood because its effects can vary, depending on experimental conditions. For example, in their comprehensive review of that drug's toxicity, Jaeschke et al. (2012) mentioned that ROS can induce an inflammatory response in immune cells, including KC, and these extracellularly generated oxidants can diffuse into hepatocytes and trigger various types of mitochondrial dysfunction and oxidant stress, which subsequently induce cell death. In addition, Botta et al. (2006) commented on the importance of glutathione synthesis by glutamate-cysteine ligase against APAP-induced liver injury using glutamate-cysteine ligase transgenic mice. On the other hand, Lewerenz et al. (2003) reported that antioxidants protect primary rat hepatocyte cultures against APAP-induced DNA strand breaks but not against APAP-induced cytotoxicity. Moreover, the knockout of Cu, Zn-superoxide dismutase, a major intracellular antioxidant enzyme, was reported to be resistant to APAP-induced hepatotoxicity (Lei et al., 2006). In this study, we demonstrated that both the pre- and postadministration of SH-Man-HSA that targets ROS derived from $CD68^+/CD206^+$ KC significantly improve the Con-A– and APAP-induced hepatopathy mouse model via the inhibition of hepatic oxidative stress. This implies that ROS derived from $CD68^+/CD206^+$ KC could be responsible for the development of liver damage in both disease models. In addition, we found that the SH-Man-HSA treatment did not significantly influence the early metabolic pathway of APAP-induced liver injury (data not shown). A similar result was also reported by Michael et al. (1999), that is, a pretreatment of $GdCl_3$ prevented APAP-induced hepatopathy without a decrease in the APAP-protein adducts. These findings indicate that ROS derived from $CD68^+/CD206^+$ KC are probably not involved in the early event of APAP toxicity and that SH-Man-HSA functions at the stage after the formation of *N*-acetyl-*p*-benzoquinone imine (NAPQI). Moreover, hypoxia-inducible factor-1α (HIF-1α) is a critical transcription factor in response to oxidative stress (James et al., 2006). It has been revealed that ROS are important contributors to the early HIF-1α stabilization that enhances APAP toxicity (Sparkenbaugh et al., 2011). Since NAC prevented HIF-1α accumulation via the inactivation of the NAPQI formation, it would be interesting to know whether SH-Man-HSA also inhibits the stabilization of HIF-1α or whether ROS derived from $CD68^+/CD206^+$ KC are involved in the HIF-1α accumulation. As mentioned above, SH-Man-HSA does not significantly influence the early metabolic pathway of APAP toxicity, SH-Man-HSA or ROS derived from KC may not be directly involved in the HIF-1α accumulation. These findings led us to conclude that, even though the early events of the onset of acute liver injury are different depending on the disease, ROS derived from $CD68^+/CD206^+$ KC might be a common contributor for the development of acute liver injury. Future investigations will be necessary to clarify these interesting issues in terms of understanding the pathologic role of ROS derived from $CD68^+/CD206^+$ KC. In addition, CD206 has been frequently used as a marker of M2 macrophages that are a type of anti-inflammatory immune cell (Choi et al., 2010). Thus, it is possible that SH-Man-HSA inhibits hepatic injury via an increase in the population of M2 macrophages. However, SH-Man-HSA did not significantly influence the balance of M1/M2 macrophages in both disease models (Supplemental Fig. 11). This indicates that the hepatoprotective effect of SH-Man-HSA is not attributable to the changes in the polarization of macrophages in liver.

Clinically, NAC is only effective if given to patients the first few hours after ingestion of an overdose of APAP. In the case of the APAP hepatotoxicity mouse model, NAC was reported to be the least beneficial if administered 3 or 4 hours after APAP injection (Saito et al., 2010). Consistent with previous reports, we also found that, even at a high dose (650 μmol SH/kg), NAC was no longer effective at 4 hours after APAP injection (Fig. 8B). Surprisingly, 20.0 μmol SH/kg of SH-Man-HSA, a dose that was approximately 33 times less than the NAC dose (650 μmol SH/kg), exhibited a significant hepatoprotective effect, even though it

was administered 4 hours later in both pathologic models. In vivo EPR data clearly showed that ROS were mainly generated in the liver at 4 to 5 hours after the injection of Con-A or APAP and was completely inhibited by SH-Man-HSA or $GdCl_3$. Taking into account the rapid and efficient delivery of SH into $CD68^+/CD206^+$ KC by SH-Man-HSA (Fig. 3) and the elevation in the hepatic SH content (Figs. 5A and 7A), these findings suggest that the difference in the therapeutic effect between SH-Man-HSA and NAC given after an injection of Con-A or APAP could be attributable to the difference in the rate and site of distribution to the liver, especially $CD68^+/CD206^+$ KC, between these two drugs.

The issue of whether the recovery of the hepatic SH content to control levels by SH-Man-HSA can be attributed to the SH moieties in SH-Man-HSA or suppression of the consumption of GSH, an intracellular substance with SH, or both, remains unknown. In contrast to the hepatic SH content, the hepatic GSH/GSSG ratio was not recovered to the control level as the result of the SH-Man-HSA treatment (Figs. 5B and 7B). Such an inconsistency might explain why, initially, GSH is consumed as the result of a Con-A or APAP challenge, and then SH derived from SH-Man-HSA makes up for the deficit in hepatic SH levels. In fact, immunohistochemical analyses (Figs. 2 and 3) and the SH levels in liver homogenates (Figs. 5A and 7A) are supportive of the hypothesis that SH liberated from SH-Man-HSA may still be retained within the liver, but not $CD68^+$ KC, at 12 hours after SH-Man-HSA administration (Fig. 3C). SH-Man-HSA would be hydrolyzed in lysosomes of $CD68^+/CD206^+$ KC after endocytosis by CD206, and the SH groups would then be liberated from SH-Man-HSA because 2-iminothiolane, the SH labeling agent for HSA used in this study, is also hydrolyzed at a low pH, such as pH 5 (Singh et al., 1996). These SH groups then move to the outside of the $CD68^+/CD206^+$ KC and would contribute to the elevation of the hepatic SH levels in disease models. Therefore, SH-Man-HSA is not only able to scavenge ROS in the liver more efficiently than NAC, but also ROS-scavenging activity is retained in the liver longer than NAC. It might be possible to treat a liver impairment with SH-Man-HSA at a lower dose and a lesser dosing frequency than is needed for NAC.

In conclusion, SH-Man-HSA is a unique and powerful nano-antioxidant that targets ROS derived from $CD68^+/CD206^+$ KC because of its efficient and rapid delivery of SH to $CD68^+/CD206^+$ KC. SH-Man-HSA exhibited an excellent hepatoprotective action against two experimental acute hepatitis models that was superior to NAC because of its sufficient suppression of oxidative stress. Therefore, it has great potential for use as a rescue therapy for acute hepatopathy. Moreover, the therapeutic impact of SH-Man-HSA in chronic hepatic diseases in which $CD68^+$ KC contribute to the onset and progression of diseases, such as in nonalcoholic steatohepatitis (Chedid et al., 2004) and alcoholic hepatitis (Gadd et al., 2014), deserves further examination.

Authorship Contributions

Participated in research design: Maeda, Hirata, Watanabe, Ishima, Inatsu, Kinoshita, Otagiri, Maruyama.

Conducted experiments: Maeda, Hirata, Tanaka, Sasaki.

Contributed new reagents or analytic tools: Maeda, Watanabe, Ishima, Inatsu, Kinoshita, Tanaka, Sasaki, Maruyama.

Performed data analysis: Maeda, Watanabe, Ishima, Inatsu, Kinoshita, Tanaka, Sasaki, Maruyama.

Wrote or contributed to the writing of the manuscript: Maeda, Watanabe, Ishima, Chuang, Taguchi, Kinoshita, Tanaka, Sasaki, Otagiri, Maruyama.

References

Ayoub SS, Botting RM, Goorha S, Colville-Nash PR, Willoughby DA, and Ballou LR (2004) Acetaminophen-induced hypothermia in mice is mediated by a prostaglandin endoperoxide synthase 1 gene-derived protein. *Proc Natl Acad Sci USA* **101**: 11165–11169.

Botta D, Shi S, White CC, Dabrowski MJ, Keener CL, Srinouanprachanh SL, Farin FM, Ware CB, Ladiges WC, Pierce RH, et al. (2006) Acetaminophen-induced liver injury is attenuated in male glutamate-cysteine ligase transgenic mice. *J Biol Chem* **281**:28865–28875.

Chedid A, Arain S, Snyder A, Mathurin P, Capron F, and Naveau S (2004) The immunology of fibrogenesis in alcoholic liver disease. *Arch Pathol Lab Med* **128**: 1230–1238.

Choi KM, Kashyap PC, Dutta N, Stoltz GJ, Ordog T, Shea Donohue T, Bauer AJ, Linden DR, Szurszewski JH, Gibbons SJ, and Farrugia G (2010) CD206-positive M2 macrophages that express heme oxygenase-1 protect against diabetic gastroparesis in mice. *Gastroenterology* **138**:2399–2409.

Dobashi H, Seki S, Habu Y, Ohkawa T, Takeshita S, Hiraide H, and Sekine I (1999) Activation of mouse liver natural killer cells and NK1.1(+) T cells by bacterial superantigen-primed Kupffer cells. *Hepatology* **30**:430–436.

Gadd VL, Skoien R, Powell EE, Fagan KJ, Winterford C, Horsfall L, Irvine K, and Clouston AD (2014) The portal inflammatory infiltrate and ductular reaction in human non-alcoholic fatty liver disease. *Hepatology* **59**:1393–1405.

Hirata K, Maruyama T, Watanabe H, Maeda H, Nakajou K, Iwao Y, Ishima Y, Katsumi H, Hashida M, and Otagiri M (2010) Genetically engineered mannosylated-human serum albumin as a versatile carrier for liver-selective therapeutics. *J Control Release* **145**:9–16.

Hnatowich DJ, Layne WW, and Childs RL (1982) The preparation and labeling of DTPA-coupled albumin. *Int J Appl Radiat Isot* **33**:327–332.

Hu W, Jiang Z, Zhang Y, Liu Q, Fan J, Luo N, Dong X, and Yu X (2012) Characterization of infiltrating macrophages in high glucose-induced peritoneal fibrosis in rats. *Mol Med Rep* **6**:93–99.

Jaeschke H (2011) Reactive oxygen and mechanisms of inflammatory liver injury: Present concepts. *J Gastroenterol Hepatol* **26** (Suppl 1):173–179.

Jaeschke H, McGill MR, and Ramachandran A (2012) Oxidant stress, mitochondria, and cell death mechanisms in drug-induced liver injury: lessons learned from acetaminophen hepatotoxicity. *Drug Metab Rev* **44**:88–106.

James LP, Mayeux PR, and Hinson JA (2003) Acetaminophen-induced hepatotoxicity. *Drug Metab Dispos* **31**:1499–1506.

James LP, Donahower B, Burke AS, McCullough S, and Hinson JA (2006) Induction of the nuclear factor HIF-1alpha in acetaminophen toxicity: evidence for oxidative stress. *Biochem Biophys Res Commun* **343**:171–176.

Katayama N, Nakajou K, Komori H, Uchida K, Yokoe J, Yasui N, Yamamoto H, Kai T, Sato M, Nakagawa T, et al. (2008) Design and evaluation of S-nitrosylated human serum albumin as a novel anticancer drug. *J Pharmacol Exp Ther* **325**: 69–76.

Kinoshita M, Uchida T, Sato A, Nakashima M, Nakashima H, Shono S, Habu Y, Miyazaki H, Hiroi S, and Seki S (2010) Characterization of two F4/80-positive Kupffer cell subsets by their function and phenotype in mice. *J Hepatol* **53**: 903–910.

Kogelberg H, Tolner B, Sharma SK, Lowdell MW, Qureshi U, Robson M, Hillyer T, Pedley RB, Vervecken W, Contreras R, et al. (2007) Clearance mechanism of a mannosylated antibody-enzyme fusion protein used in experimental cancer therapy. *Glycobiology* **17**:36–45.

Korenaga M, Wang T, Li Y, Showalter LA, Chan T, Sun J, and Weinman SA (2005) Hepatitis C virus core protein inhibits mitochondrial electron transport and increases reactive oxygen species (ROS) production. *J Biol Chem* **280**:37481–37488.

Kragh-Hansen U, Donaldson D, and Jensen PH (2001) The glycan structure of albumin Redhill, a glycosylated variant of human serum albumin. *Biochim Biophys Acta* **1550**:20–26.

Laskin DL and Laskin JD (2001) Role of macrophages and inflammatory mediators in chemically induced toxicity. *Toxicology* **160**:111–118.

Laskin DL, Gardner CR, Price VF, and Jollow DJ (1995) Modulation of macrophage functioning abrogates the acute hepatotoxicity of acetaminophen. *Hepatology* **21**: 1045–1050.

Lee WM, Squires RH, Jr, Nyberg SL, Doo E, and Hoofnagle JH (2008) Acute liver failure: Summary of a workshop. *Hepatology* **47**:1401–1415.

Lei XG, Zhu JH, McClung JP, Aregullin M, and Roneker CA (2006) Mice deficient in Cu,Zn-superoxide dismutase are resistant to acetaminophen toxicity. *Biochem J* **399**:455–461.

Lewerenz V, Hanelt S, Nastevska C, El-Bahay C, Röhrdanz E, and Kahl R (2003) Antioxidants protect primary rat hepatocyte cultures against acetaminophen-induced DNA strand breaks but not against acetaminophen-induced cytotoxicity. *Toxicology* **191**:179–187.

McGreal EP, Rosas M, Brown GD, Zamze S, Wong SY, Gordon S, Martinez-Pomares L, and Taylor PR (2006) The carbohydrate-recognition domain of Dectin-2 is a C-type lectin with specificity for high mannose. *Glycobiology* **16**:422–430.

Michael SL, Pumford NR, Mayeux PR, Niesman MR, and Hinson JA (1999) Pretreatment of mice with macrophage inactivators decreases acetaminophen hepatotoxicity and the formation of reactive oxygen and nitrogen species. *Hepatology* **30**:186–195.

Minchiotti L, Campagnoli M, Rossi A, Cosulich ME, Monti M, Pucci P, Kragh-Hansen U, Granel B, Disdier P, Weiller PJ, et al. (2001) A nucleotide insertion and frameshift cause albumin Kénitra, an extended and O-glycosylated mutant of

human serum albumin with two additional disulfide bridges. *Eur J Biochem* **268**: 344–352.
Moreno-Otero R (2013) May oxidative stress contribute to autoimmune hepatitis pathogenesis, and can antioxidants be of value as adjuvant therapy for refractory patients? *Dig Dis Sci* **58**:1440–1441.
Nakashima H, Kinoshita M, Nakashima M, Habu Y, Shono S, Uchida T, Shinomiya N, and Seki S (2008) Superoxide produced by Kupffer cells is an essential effector in concanavalin A-induced hepatitis in mice. *Hepatology* **48**:1979–1988.
Roberts RA, Ganey PE, Ju C, Kamendulis LM, Rusyn I, and Klaunig JE (2007) Role of the Kupffer cell in mediating hepatic toxicity and carcinogenesis. *Toxicol Sci* **96**: 2–15.
Sato K, Kadiiska MB, Ghio AJ, Corbett J, Fann YC, Holland SM, Thurman RG, and Mason RP (2002) In vivo lipid-derived free radical formation by NADPH oxidase in acute lung injury induced by lipopolysaccharide: a model for ARDS. *FASEB J* **16**:1713–1720.
Saito C, Zwingmann C, and Jaeschke H (2010) Novel mechanisms of protection against acetaminophen hepatotoxicity in mice by glutathione and N-acetylcysteine. *Hepatology* **51**:246–254.
Singh R, Kats L, Blättler WA, and Lambert JM (1996) Formation of N-substituted 2-iminothiolanes when amino groups in proteins and peptides are modified by 2-iminothiolane. *Anal Biochem* **236**:114–125.
Sparkenbaugh EM, Saini Y, Greenwood KK, LaPres JJ, Luyendyk JP, Copple BL, Maddox JF, Ganey PE, and Roth RA (2011) The role of hypoxia-inducible factor-1α in acetaminophen hepatotoxicity. *J Pharmacol Exp Ther* **338**:492–502.
Sun H, Xu XY, Shao HT, Su X, Wu XD, Wang Q, and Shi Y (2013) Dectin-2 is predominately macrophage restricted and exhibits conspicuous expression during Aspergillus fumigatus invasion in human lung. *Cell Immunol* **284**:60–67.
Tsukamoto H and Lu SC (2001) Current concepts in the pathogenesis of alcoholic liver injury. *FASEB J* **15**:1335–1349.

Address correspondence to: Dr. Toru Maruyama, Department of Biopharmaceutics, Graduate School of Pharmaceutical Sciences, Kumamoto University, 5-1 Oe-honmachi, Kumamoto 862-0973, Japan. E-mail: tomaru@gpo.kumamoto-u.ac.jp

Hum Genet (2015) 134:279–289
DOI 10.1007/s00439-014-1520-7

ORIGINAL INVESTIGATION

Genome-wide association study identifies a *PSMD3* variant associated with neutropenia in interferon-based therapy for chronic hepatitis C

Etsuko Iio · Kentaro Matsuura · Nao Nishida · Shinya Maekawa · Nobuyuki Enomoto · Mina Nakagawa · Naoya Sakamoto · Hiroshi Yatsuhashi · Masayuki Kurosaki · Namiki Izumi · Yoichi Hiasa · Naohiko Masaki · Tatsuya Ide · Keisuke Hino · Akihiro Tamori · Masao Honda · Shuichi Kaneko · Satoshi Mochida · Hideyuki Nomura · Shuhei Nishiguchi · Chiaki Okuse · Yoshito Itoh · Hitoshi Yoshiji · Isao Sakaida · Kazuhide Yamamoto · Hisayoshi Watanabe · Shuhei Hige · Akihiro Matsumoto · Eiji Tanaka · Katsushi Tokunaga · Yasuhito Tanaka

Received: 2 October 2014 / Accepted: 8 December 2014 / Published online: 17 December 2014

Abstract Cytopenia during interferon-based (IFN-based) therapy for chronic hepatitis C (CHC) often necessitates reduction of doses of drugs and premature withdrawal from therapy resulting in poor response to treatment. To identify genetic variants associated with IFN-induced neutropenia, we conducted a genome-wide association study (GWAS) in 416 Japanese CHC patients receiving IFN-based therapy. Based on the results, we selected 192 candidate single nucleotide polymorphisms (SNPs) to carry out a replication analysis in an independent set of 404 subjects. The SNP rs2305482, located in the intron region of the *PSMD3* gene on chromosome 17, showed a strong association when the results of GWAS and the replication stage were combined (OR = 2.18, $P = 3.05 \times 10^{-7}$ in the allele frequency model). Logistic regression analysis showed that rs2305482 CC and neutrophil count at baseline were independent predictive factors for IFN-induced neutropenia (OR = 2.497, $P = 0.0072$ and OR = 0.998, $P < 0.0001$, respectively). Furthermore, rs2305482 genotype was associated with the doses of pegylated interferon (PEG-IFN) that could be tolerated in hepatitis C virus genotype 1-infected patients treated with PEG-IFN plus ribavirin, but not with treatment efficacy. Our results suggest that genetic

E. Iio and K. Matsuura equally contributed to this work (shared first authorship).

Electronic supplementary material The online version of this article (doi:10.1007/s00439-014-1520-7) contains supplementary material, which is available to authorized users.

E. Iio · K. Matsuura · Y. Tanaka (✉)
Department of Virology and Liver Unit, Nagoya City University Graduate School of Medical Sciences, Kawasumi, Mizuho, Nagoya 467-8601, Japan
e-mail: ytanaka@med.nagoya-cu.ac.jp

E. Iio · K. Matsuura
Department of Gastroenterology and Metabolism, Nagoya City University Graduate School of Medical Sciences, Nagoya 467-8601, Japan

N. Nishida · N. Masaki
The Research Center for Hepatitis and Immunology, National Center for Global Health and Medicine, Ichikawa 272-8516, Japan

N. Nishida · K. Tokunaga
Department of Human Genetics, Graduate School of Medicine, The University of Tokyo, Tokyo 113-0033, Japan

S. Maekawa · N. Enomoto
First Department of Internal Medicine, University of Yamanashi, Chuo 409-3898, Japan

M. Nakagawa · N. Sakamoto
Department of Gastroenterology and Hepatology, Tokyo Medical and Dental University, Tokyo 113-0034, Japan

N. Sakamoto · S. Hige
Department of Internal Medicine, Hokkaido University Graduate School of Medicine, Sapporo 060-0814, Japan

H. Yatsuhashi
Clinical Research Center, National Nagasaki Medical Center, Omura 856-8562, Japan

M. Kurosaki · N. Izumi
Division of Gastroenterology and Hepatology, Musashino Red Cross Hospital, Musashino 180-0023, Japan

testing for this variant might be useful for establishing personalized drug dosing in order to minimize drug-induced adverse events.

Introduction

Chronic hepatitis C virus (HCV) infection is a significant risk factor for progressive liver fibrosis and hepatocellular carcinoma. Antiviral treatment improves the natural course in chronic hepatitis C (CHC) (George et al. 2009; Yoshida et al. 2004). Newly-developed treatments involving direct-acting antivirals (DAAs), including nonstructural (NS) 3/4A protease inhibitors have shown promising outcomes in combination with pegylated interferon (PEG-IFN) plus ribavirin (RBV) in several clinical trials. Thus, >70 % of patients infected with HCV genotype 1 are reported to achieve sustained virological responses (SVR) (Jacobson et al. 2011; Poordad et al. 2012; Zeuzem et al. 2011). Furthermore, interferon-free (IFN-free) therapies are expected to be useful especially in IFN-resistant patients and may become the standard of care in the near future. However, IFN-based regimens have been standard-of-care therapies over the last couple of decades.

IFN-based therapies are associated with various adverse effects. Cytopenia is common due to bone marrow suppression cased by IFN or DAA and hemolysis by RBV. This is particularly the case in patients with advanced hepatic fibrosis, but can sometimes also occur in those with mild fibrosis. This then often necessitates dose reduction or premature withdrawal from therapy, resulting in poor response to treatment. For instance, it was reported that rates of viral clearance were significantly reduced in patients who could not be maintained on at least 80 % of their drug doses for the duration of PEG-IFN/RBV therapy (McHutchison et al. 2002). Therefore, pre-treatment prediction of possible adverse effects in order to avoid them and undergo therapy safely is desirable.

Recent genome-wide association studies (GWASs) have identified two important host genetic variants influencing CHC treatment: (1) single nucleotide polymorphisms (SNPs) near the interleukin-28B (*IL28B*) gene, which are strongly associated with response to therapy for chronic HCV genotype 1 infection (Ge et al. 2009; Suppiah et al. 2009; Tanaka et al. 2009), and (2) SNPs in the inosine triphosphatase (*ITPA*) gene, which accurately predict RBV-induced anemia in European–American (Fellay et al. 2010) and Japanese population (Ochi et al. 2010). We validated the association between this *ITPA* genetic variant and RBV-induced anemia (Sakamoto et al. 2010), and reported that the *ITPA* genotype affects the tolerated doses of RBV and treatment response in a stratified group (Kurosaki et al. 2011; Matsuura et al. 2014). Additionally, our GWAS showed that *DDRGK1/ITPA* variants are strongly associated with IFN-induced thrombocytopenia as well as anemia during PEG-IFN/RBV therapy (Tanaka et al. 2011). Thompson et al. (2012) also reported that the *ITPA* genetic variant was associated with anemia and thrombocytopenia during PEG-IFN/RBV therapy. However they identified no genetic determinants of IFN-induced neutropenia at the level of genome-wide significance by their GWAS in populations of European Americans, African Americans and Hispanics.

Hence, to identify genetic variants associated with IFN-induced neutropenia, we conducted a GWAS in Japanese CHC patients.

Y. Hiasa
Department of Gastroenterology and Metabology, Ehime University Graduate School of Medicine, Toon 791-0295, Japan

T. Ide
Division of Gastroenterology, Department of Medicine, Kurume University, Kurume 830-0011, Japan

K. Hino
Department of Hepatology and Pancreatology, Kawasaki Medical School, Kurashiki 701-0114, Japan

A. Tamori
Department of Hepatology, Osaka City Graduate School of Medicine, Osaka 545-8585, Japan

M. Honda · S. Kaneko
Department of Gastroenterology, Kanazawa University Graduate School of Medicine, Kanazawa 920-0934, Japan

S. Mochida
Division of Gastroenterology and Hepatology, Internal Medicine, Saitama Medical University, Iruma 350-0495, Japan

H. Nomura
The Center for Liver Disease, Shin-Kokura Hospital, Kitakyushu 803-8505, Japan

S. Nishiguchi
Department of Internal Medicine, Hyogo College of Medicine, Nishinomiya 663-8131, Japan

C. Okuse
Department of Gastroenterology and Hepatology, St. Marianna University School of Medicine, Kawasaki 216-8511, Japan

Y. Itoh
Molecular Gastroenterology and Hepatology, Kyoto Prefectural University of Medicine, Kyoto 602-0841, Japan

H. Yoshiji
Third Department of Internal Medicine, Nara Medical University, Kashihara 634-8522, Japan

I. Sakaida
Department of Gastroenterology and Hepatology, Yamaguchi University Graduate School of Medicine, Ube 755-8505, Japan